RESULTS AND DISCUSSION

1. Catalyst Preparation

The samples obtained from the Pechini, the Schiff base complex and the coprecipitation methods were assigned as LC-PN, LC-SB and LC-CP, respectively. Thermal behaviors of the as prepared samples from the three methods were studied by TGA and FTIR. XRD was used for investigation the perovskite crystallinity.

1.1 The Pechini method (PN)

1.1.1 Thermogravimetric analysis (TGA)

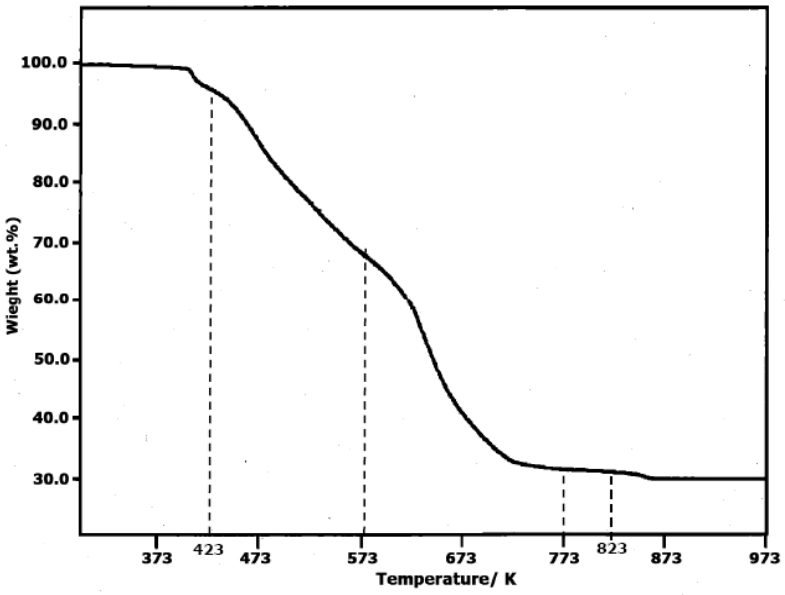

Figure 32 TG curve of the sample prepared by the Pechini method

A TG curve of the dried gel obtained by the Pechini method is shown in Figure 32. The TG curve showed a small weight loss up to 423 K, followed by a major weight loss up to 773 K. A small kink presented at 823 K, which no further weight loss up to 873 K. To explain the weight loss of each step, FTIR of the

prepare gel was studied. The first weight loss could be ascribed to the decomposition and burnout of the organics trapped in the powder precursor [Figure 37(a – c)]. The second large weight loss between 423 and 773 K could be ascribed to the decomposition of most of the organics trapped in the powder precursor and formation of an intermediate decomposition product [Figure 37(d – h)]. The weak weight loss at 823 K was corresponded to carbonates that were involved in the intermediate product decomposed to obtain the $LaCoO_3$ perovskite [Figure 37(i)].

1.1.2 Fourier Transform Infrared Spectroscopy (FTIR)

IR spectra of the Pechini samples dried at 383 K are reported in Table 11 and shown in Figure 33.

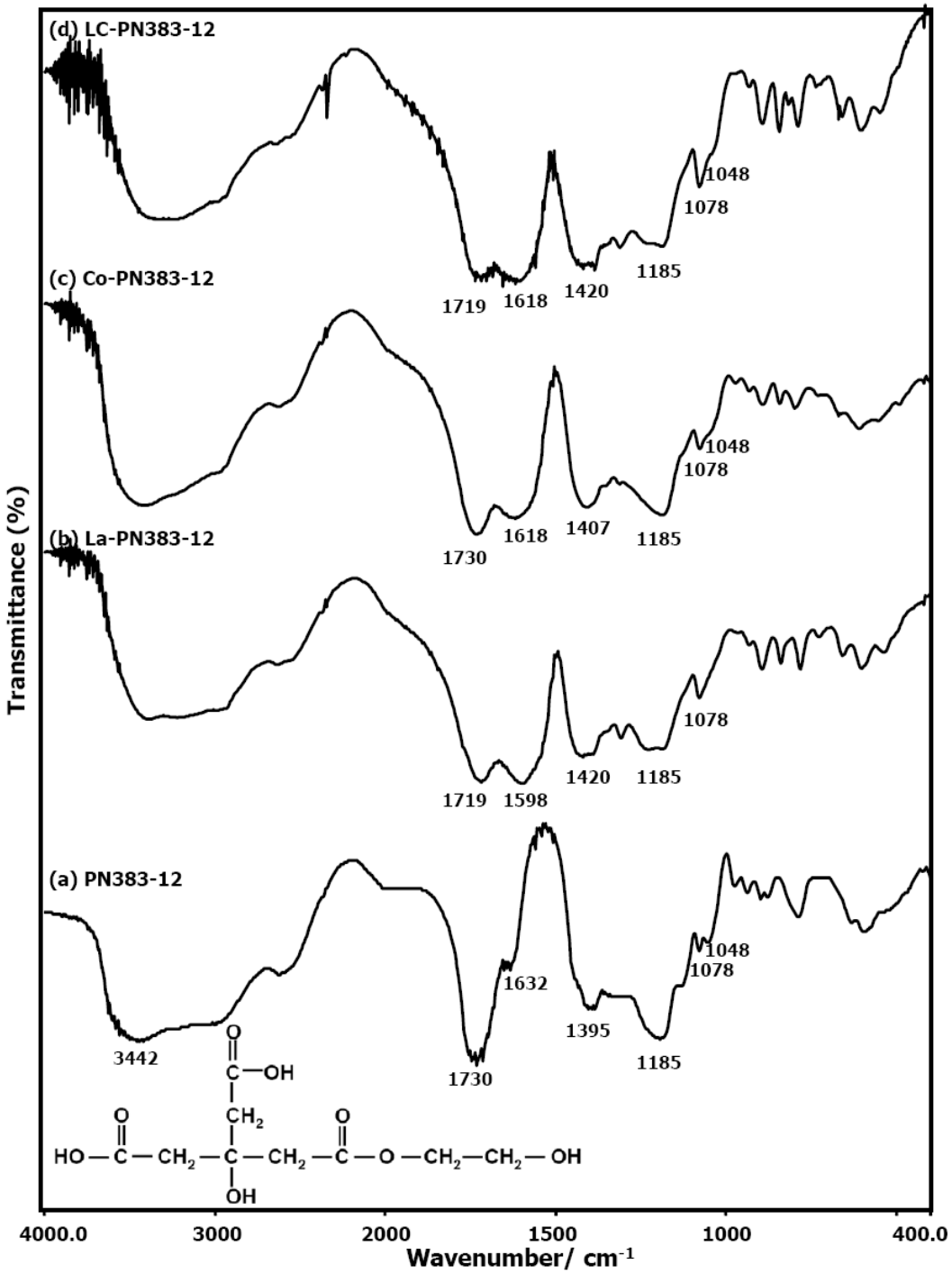

Figure 33 FTIR spectra of the samples prepared by the Pechini method at 383 K (a) PN383-12, (b) La-PN383-12, (c) Co-PN383-12 and (d) LC-PN383-12

Table 11 FTIR spectra assignment of samples prepared by the Pechini method

Functional group / Catalysts	Wavenumber (cm^{-1})								
	O–H stretching	C=O stretching	C–O stretching of resonance carbonyl	C–O stretching of alcohol	C–C stretching of ester	C–O stretching of ester	N–O bending of nitrate ion	C–O carbonate	Co–O stretching
Reference	~3400[a]	1725[a]	1600[b]	1380[b]	1180[b]	1086 1043[c]	1384[d]	1460 1060 860[a]	596 552[e]
PN383-12	3442	1730	1632	1395	1185	1078 1048	-	-	-
La-PN383-12		1719	1598	1420	1185	1078 1048	1384	-	-
Co-PN383-12		1730	1618	1407	1185	1078 1048	1384	-	-
LC-PN383-12	3442	1719	1618	1420	1185	1078 1048	1384	-	-
LC-PN523-03	-	-	-	-	1185	-	1384	1476 1066 844	584
LC-PN773-08	-	-	-	-	1185	-	1384	1476 1066 844	593 551

[a] Yang *et al*. (2006) [b] Wang *et al*. (2006) [c] Sinquin *et al*. (2001) [d] Nishizawa and Katsube (1997) [e] Khalil (2003)

In the Pechini method, citric acid was used to chelate metal ions and ethylene glycol was used as solvent for polymerization via polyester formation according to a proposed mechanism shown in Figure 34. Co nitrate dissolves in water producing Co^{2+} ion and nitrate ion. After the addition of citric acid, Co-citrate complex and two nitric acid ions are formed. Then La^{3+} ion obtained from La nitrate dissolving in water is added to form La/Co-citrate complex.

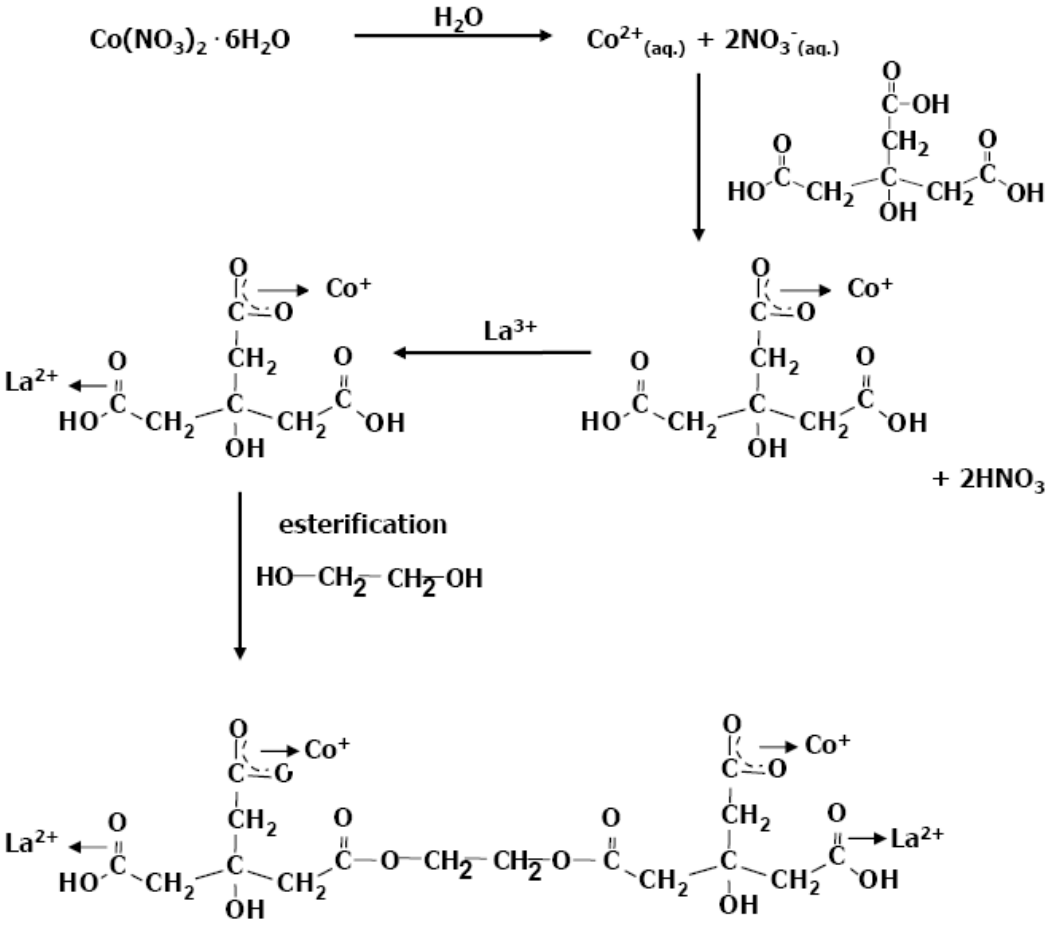

Figure 34 The proposed mechanism of the Pechini method

Ethylene glycol greatly inhibited metal ions segregation and achieved a homogeneous precursor in the polymerization of citric acid-metal complexes (Sinquin *et al.*, 2001).

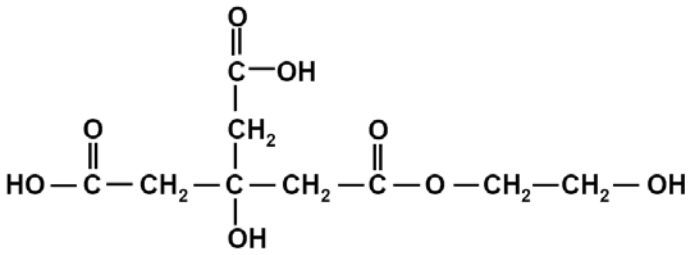

Figure 35 The proposed structure of the ester resulted from the reaction of citric acid and ethylene glycol

IR spectra of PN precursor (PN383-12) in Figure 33(a) appeared a broad band around 3400 cm^{-1} as the characteristic of absorbed water or hydroxyl group in alcohol. The 1730 cm^{-1} band was C=O stretching of uncoordinated carboxylic group compared to 1725 cm^{-1} as reported by Wang *et al.*, 2006. The bands at 1632 and 1395 cm^{-1} were contributed to the vibrations of the resonance carbonyl groups. La-PN383-12 in Figure 33(b) exhibited those bands at 1719, 1598 and 1420 cm^{-1} shifted from 1730, 1632 and 1395 cm^{-1}, respectively. In Figure 33(c), Co-PN383-12 exhibited those bands at 1730, 1618 and 1407 cm^{-1}. Those peaks contribute to the vibrations of the resonance carbonyl groups (Yang *et al.*, 2005), revealed that the carboxylate of citric acid have coordinated to lanthanum and cobalt ion precursors. LC-PN383-12, Figure 33(d), showed the bands shifted to 1719, 1618 and 1420 cm^{-1} indicating the complexation of cobalt and lanthanum ions to C=O of the carboxyl group in citric acid [Figure 36(a)] and carboxylates [Figure 36(b), 36(c)]. Strong absorption bands appeared at 1078 and 1048 cm^{-1} attributed to the C–O stretching from ethylene glycol in the polymerization process (Nishizawa *et al.*, 1997).

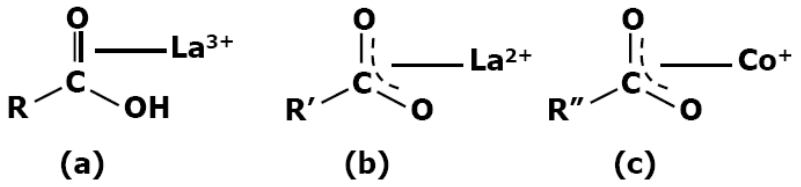

Figure 36 The complexation of the metal ions with the carboxylate in precursor prepared by the Pechini method

Figure 37 shows the FTIR spectra of the dried samples after heat–treatment from 383 to 973 K. The spectra of the resin dried at 383 K shown in Figure 37(a), exhibited a broad adsorption band around 3400 cm^{-1} which was the characteristic of absorbed water or hydroxyl group in alcohol. It also showed the sharp absorption bands at the vicinities of 1719 cm^{-1}, which can be attributed to the monodentate linkage carbonyl groups (COO^{-}) to the metal ion. There were two absorption bands at 1609 and 1406 cm^{-1}, which were due to asymmetric and symmetric vibration of the resonance carbonyl groups (Yang *et al*., 2005). The absorption band at 1384 cm^{-1} was corresponded to nitrate (Sinquin *et al*., 2001). The absorption bands appeared at 1185 cm^{-1}, attributed to the C–C stretching, and at 1078 and 1048 cm^{-1} were attributed to the C–O stretching, of ethylene glycol in the polymerization. The resin was appeared to exhibit both monodentate and bidentate ligand of carbonyl group, indicating the chelating of carbonyl group to metal ions.

In Figure 37(a) – 37(c), the intensities of the characteristic bands of carbonyl bidentate ligands showed two strong absorption bands at 1609 and 1406 cm^{-1} which did not change much during the heat treatment below 473 K. Whereas the monodentate ligands of COO^{-} and C–C–O structure were decreased dramatically. After treatment at 523 K, Figure 37(d), the characteristic stretching vibration peaks of carbonyl group at 1476, 1066 and 844 cm^{-1} revealed the existence of carbonates. As the dried gel calcined above 773 K, Figure 37(h), the 1476, 1066 and 844 cm^{-1} absorption peak disappeared, indicating the decomposition of carbonate. (Yang *et al*., 2005)

Additionally, the wide absorption band at 584 cm^{-1} of the gel calcined at 573 K [Figure 37(e)], suggested Co–O formation. When the calcination temperature was increased to 773 K, this band splits 593, 554 cm^{-1} due to Co–O stretching in the $LaCoO_3$ [Figure 37(g)]. According to the trivalent Co ions in $LaCoO_3$ were divided into two different species Co(I)–O and Co(II)–O band distances which dominate the magnitude of the stretching vibration frequencies (Khalil, 2003). After

calcination at 823 K [Figure 37(i)], only characteristic band of Co–O stretching was observed with no absorption peaks of the organic network.

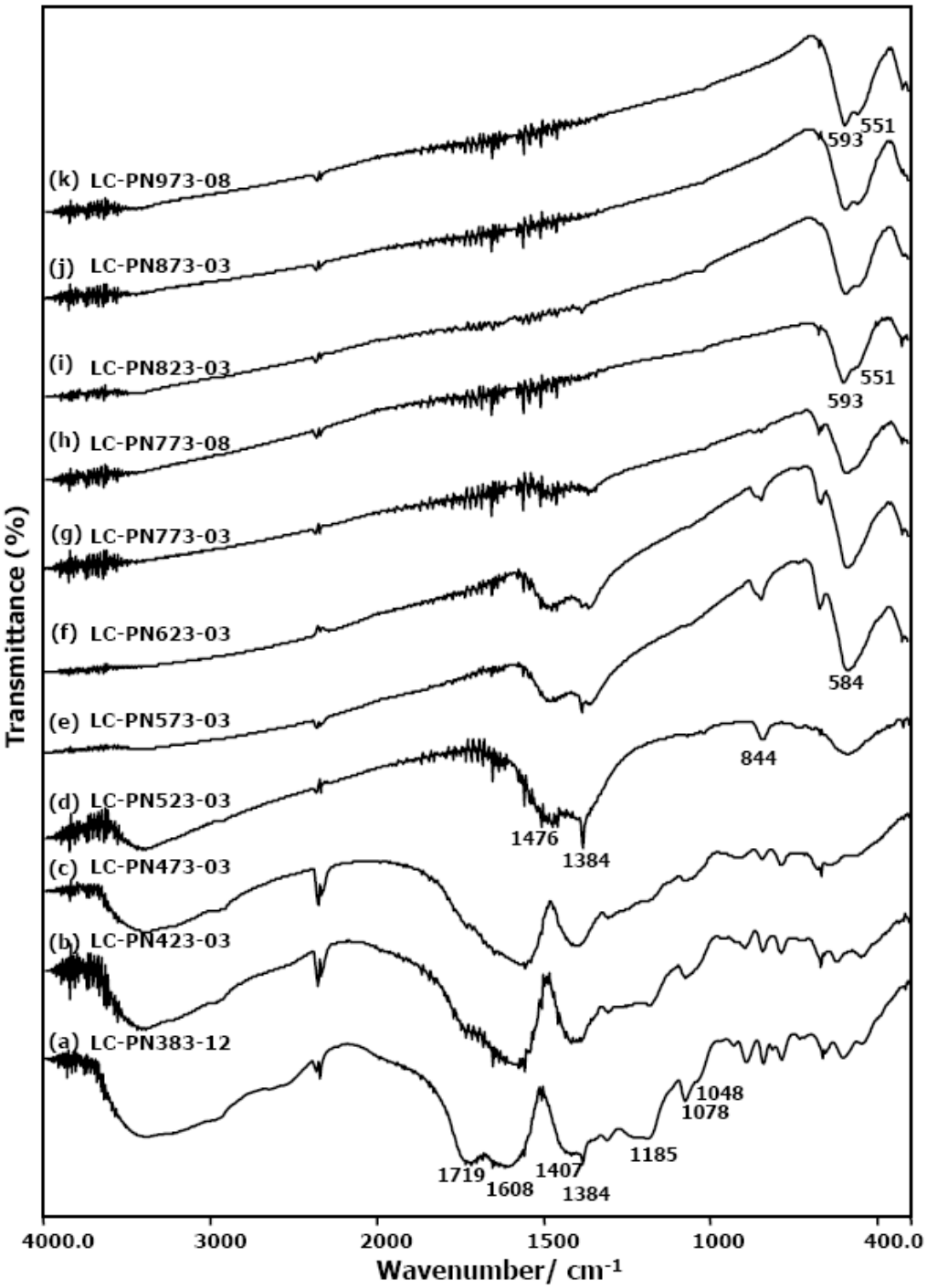

Figure 37 FTIR spectra of the samples prepared by the Pechini method at various temperatures

1.1.3 X-ray Powder diffraction (XRD)

Diffraction data in Table 12 belong to the first peaks having the highest intensity of reference and prepared $LaCoO_3$ catalysts of which XRD patterns are displayed in Figure 38.

Table 12 Diffraction data of $LaCoO_3$ reference and $LaCoO_3$ prepared by the Pechini method

Catalysts	2θ	I/I_0	d
$LaCoO_3$	32.91	100	2.72
(JCPDS no: 25-1060)	33.31	95	2.69
	47.52	70	1.91
	59.01	55	1.56
LC-PN573-03	33.28	100.00	2.69
	47.53	49.65	1.91
	58.91	56.78	1.57
LC-PN773-08	33.24	100.00	2.69
	47.56	52.48	1.91
	58.94	46.54	1.56
LC-PN823-08	33.00	100.00	2.71
	47.65	60.54	1.91
	59.04	53.15	1.56
LC-PN973-08	33.02	93.54	2.71
	33.27	100.00	2.69
	47.54	63.54	1.91

The XRD pattern in Figure 38 resulted from the Pechini method showed mainly the $LaCoO_3$ perovskite phase around 2θ 32.91°, 33.01° and 47.52° (JCPDS No. 25-1060).

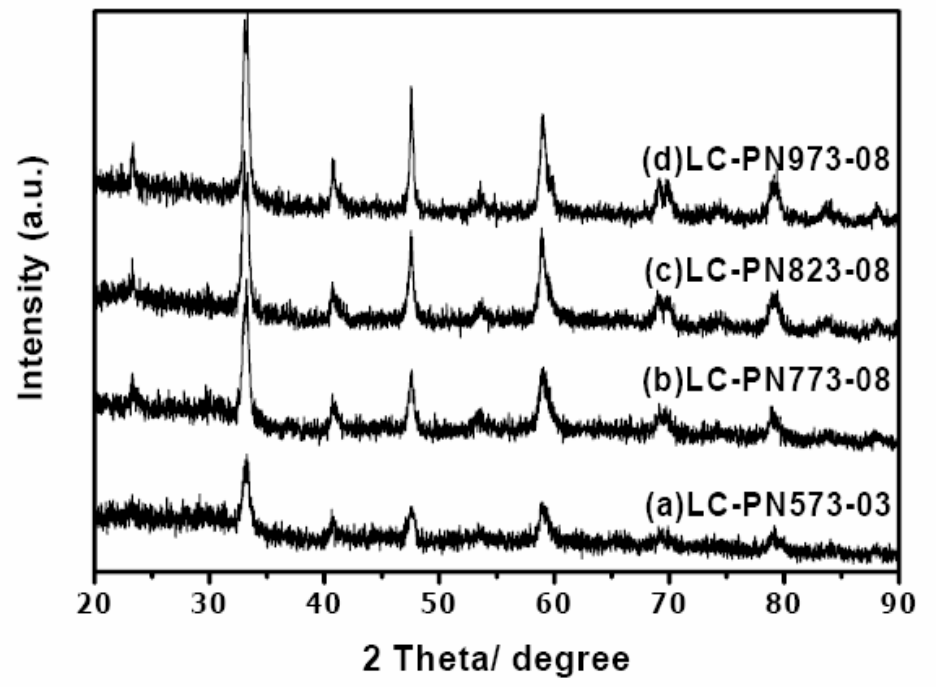

Figure 38 X-ray diffraction patterns of the samples prepared by the Pechini method and calcined at various temperatures (a) LC-PN573-03, (b) LC-PN773-08, (c) LC-PN823-08 and (d) LC-PN973-08

The powder calcined at 573 K for 3 hours [Figure 38(a)] with intensive diffraction peaks indicated that the powder was a structure of $LaCoO_3$. The results revealed some amorphous of the material after calcination at this temperature. After thermal treatment for 8 hours at 773 K, Figure 38(b), a poorly crystallized monophase material corresponding to rhombohedral $LaCoO_3$ perovskite was formed. Well-resolved x-ray patterns were obtained from powders calcined at 823 K and 973 K clearly suggested the formation of a highly crystallized powder [Figure 38(c) and 38(d)].

The calculated value of crystallite size of each calcined samples are shown in Table 13 and the calculation details are shown as follows:

At (h k l) = (0 2 4); $2\theta = 47.62^{\circ}$, thus calculated value of $\beta_{reference}$ due to equation 15 is as follow:

$$\beta_{reference} = 0.0027\, e^{-8\times10^{-4}\times 47.62}$$

$$\beta_{reference} = 2.60\times10^{-3} \text{ radian}$$

The value of FWHM 1.18˚ must be changed into radian unit using observed scale value of 1˚= π/ 180˚ radian. Thus

$$\beta_{observed} = 1.18^\circ \times \frac{\pi}{180^\circ}$$

$$\beta_{observed} = 2.05\times10^{-2} \text{ radian}$$

The true peak breadth, β, in radian unit is given by;

$$\beta = \sqrt{\left(2.05\times10^{-2}\right)^2 - \left(2.60\times10^{-3}\right)^2}$$

$$\beta = 2.04\times10^{-2} \text{ radian} \qquad \text{.....(16)}$$

Substitute the value of β in equation 16, k = 0.9 and λ = 1.54 Å into Scherrer equation and crystallite size (D) can be determined as follows:

$$D = \frac{(0.9)(1.54)}{2.04\times10^{-2}\cos 0.42}$$

$$D = 74.52 \text{ Å}$$

$$D = 7.5 \text{ nm}$$

The crystallite size of the calcined powder at 573 K was 7.5 nm by means of x-ray broadening method using Scherrer equations. With increasing temperature, the intensity of peaks gradually increased and sharpened with no change of location. The crystalline size also increased. The calculated values of crystallite sizes of PN samples are summarized in Table 13.

Table 13 Calculated values of crystallite sizes of samples prepared by the Pechini method

Catalysts	2Theta	Theta (radian)	β_s (radian)	FWHM β_m (degree)	β_m (radian)	β (radian)	D (nm)
LC-PN573-03	47.62	0.4156	0.0026	1.18	0.0205	0.0204	7.5
LC-PN773-08	47.58	0.4153	0.0026	0.72	0.0126	0.0123	12.3
LC-PN823-08	47.60	0.4154	0.0026	0.49	0.0086	0.0082	18.6
LC-PN973-08	47.52	0.4147	0.0026	0.42	0.0073	0.0068	22.3

1.2 Schiff base complex method (SB)

1.2.1 Thermogravimetric analysis (TGA)

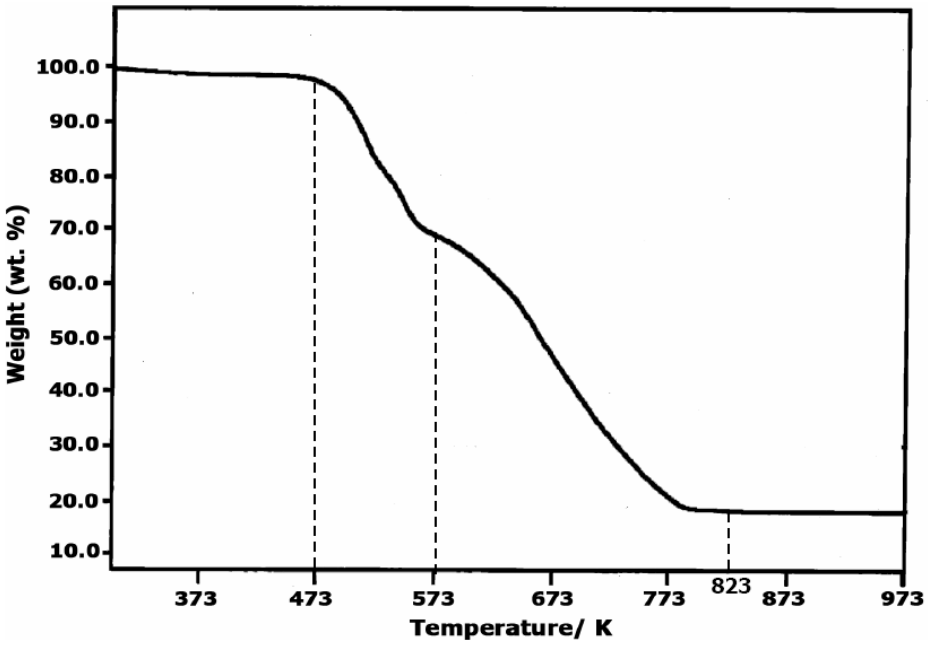

Figure 39 TG curve of the sample prepared by Schiff base complex method

A TG curve of the powder precursor obtained by Schiff base complex method is shown in Figure 39. To explain the weight loss of each step, FTIR of the

prepare gel was studied. The former weight loss at a range of 473 – 573 K indicated that the organic precursors decomposed to form intermediate species [Figure 43(c – e)]. The latter of thermogram showed continuous weight loss between 573 – 823 K due to burnout of carbonates trapped in the powder precursor until the formation of respective perovskite oxide [Figure 43(e – i)].

1.2.2 Fourier Transform Infrared Spectroscopy (FTIR)

FTIR spectra of the dried samples prepared by Schiff base complex method are shown in Figure 40 and are summarized in Table 14.

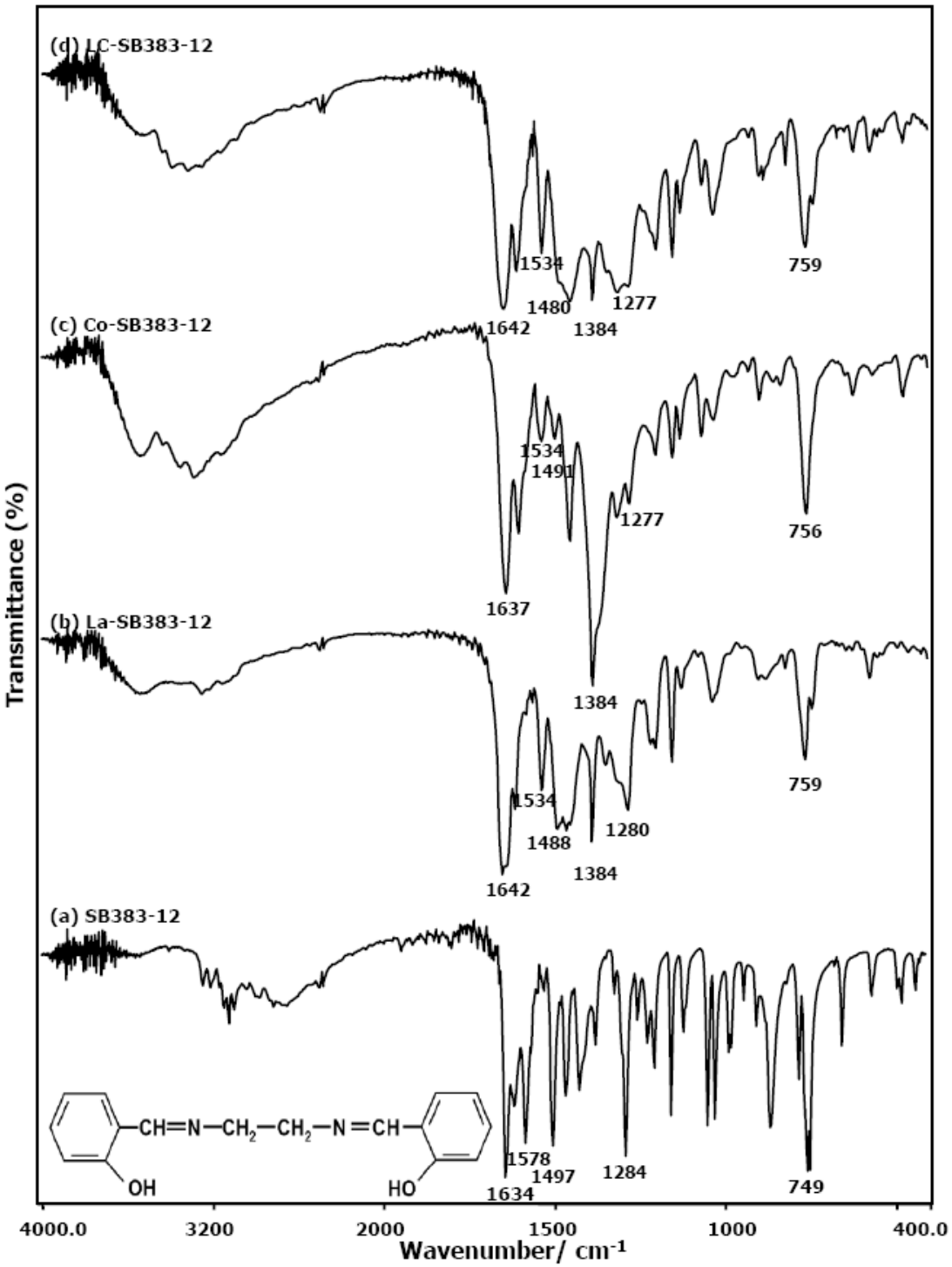

Figure 40 FTIR spectra of the samples prepared by Schiff base complex method at 383 K (a) SB383-12, (b) La-SB383-12, (c) Co-SB383-12 and (d) LC-SB383-12

Table 14 FTIR spectra assignment of samples prepared by Schiff base complex method

Functional group / Catalysts	Wavenumber (cm^{-1})						
	C=N stretching	C=C stretching	C–O stretching	C–H out of plane bending	N–O bending of nitrate ion	C–O carbonate	Co–O stretching
Reference	1634[(a)]	1578 1498[(a)]	1284[(a)]	751[(a)]	1384[(b)]	1460 1060 860[(c)]	596 552[(d)]
SB383-12	1634	1578 1497	1284	743	-	-	-
La-SB383-12	1642	1578 1488	1280	759	1384	-	-
Co-SB383-12	1637	1578 1491	1277	756	1384	-	-
LC-SB383-12	1642	1578 1480	1277	759	1384	-	-
LC-SB523-03	-	-	-	-	1384	1476 1066 844	586
LC-SB773-08	-	-	-	-	1384	1476 1066 844	598 554

[(a)] Poucher (1985) [(b)] Sinquin *et al.* (2001) [(c)] Yang *et al.* (2006) [(d)] Khalil (2003)

The Schiff base was formed from salicylaldehyde and ethylene diamine before the complexation as shown by the spectra of SB383-12 in Figure 40(a).

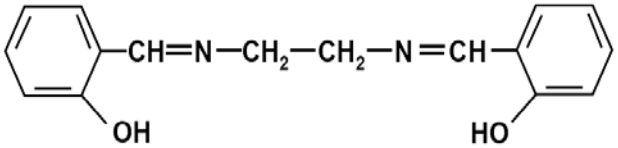

Figure 41 The proposed structure of the resulted Schiff base

The IR spectra of SB383-12 exhibited multiple bands 2900 cm^{-1} due to the presence of neat ethylene group. The strong C=N stretching of imine group appeared at 1634 cm^{-1}. The absorption band at 1578 and 1497 cm^{-1} attributed to C=C stretching, 1284 and 749 cm^{-1} attributed to C–O stretching and C–H out of plane bending of aromatic ring, respectively. La-SB383-12 [Figure 40(b)] showed a significant shift of the C=N stretching band to 1642 cm^{-1} indicated the coordination of azomethine nitrogen (C=N) of the Schiff base to lanthanum corresponding to the result in (Kaczmarek *et al.*, 2004). The strong band at 1284 cm^{-1} of C-O bond in Schiff base has decreased in intensity and shifted a little bit to 1280 cm^{-1} which indicated that lanthanum ion did not strongly coordinate to –OH substituent on the aromatic ring of the Schiff base which could be proposed by the structure in Figure 42(a). In Figure 40(c) of Co-SB383-12 showed no change of C=N stretching in the Schiff base at 1637 cm^{-1} and the strong band at 1284 cm^{-1} of C–O bond in Schiff base has shifted to 1277cm^{-1} which indicated that cobalt ion coordinated to –OH functional group of the Schiff base with no interaction with C=N [Figure 42(b)]. The infrared spectra of LC-SB383-12 in Figure 40(d) indicated that C=N was coordinated to lanthanum ion with the stretching frequency shifting to 1642 cm^{-1} and –OH substituent on the aromatic ring of the Schiff base was coordinated to cobalt ion shifting to 1277 cm^{-1}.

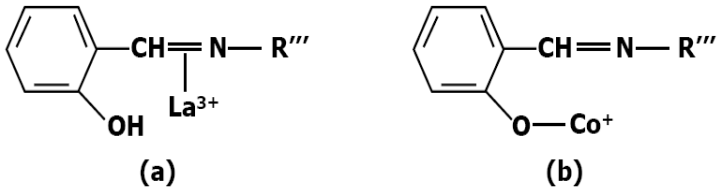

Figure 42 The complexation of the metal ions with the azomethine in precursor prepared by Schiff base complex

In an attempt to better understand what phases are formed once the volatile component was expelled, an experiment was performed whereby the dried samples were calcined at several temperatures up to 973 K followed by FTIR analysis. These results are illustrated in Figure 43.

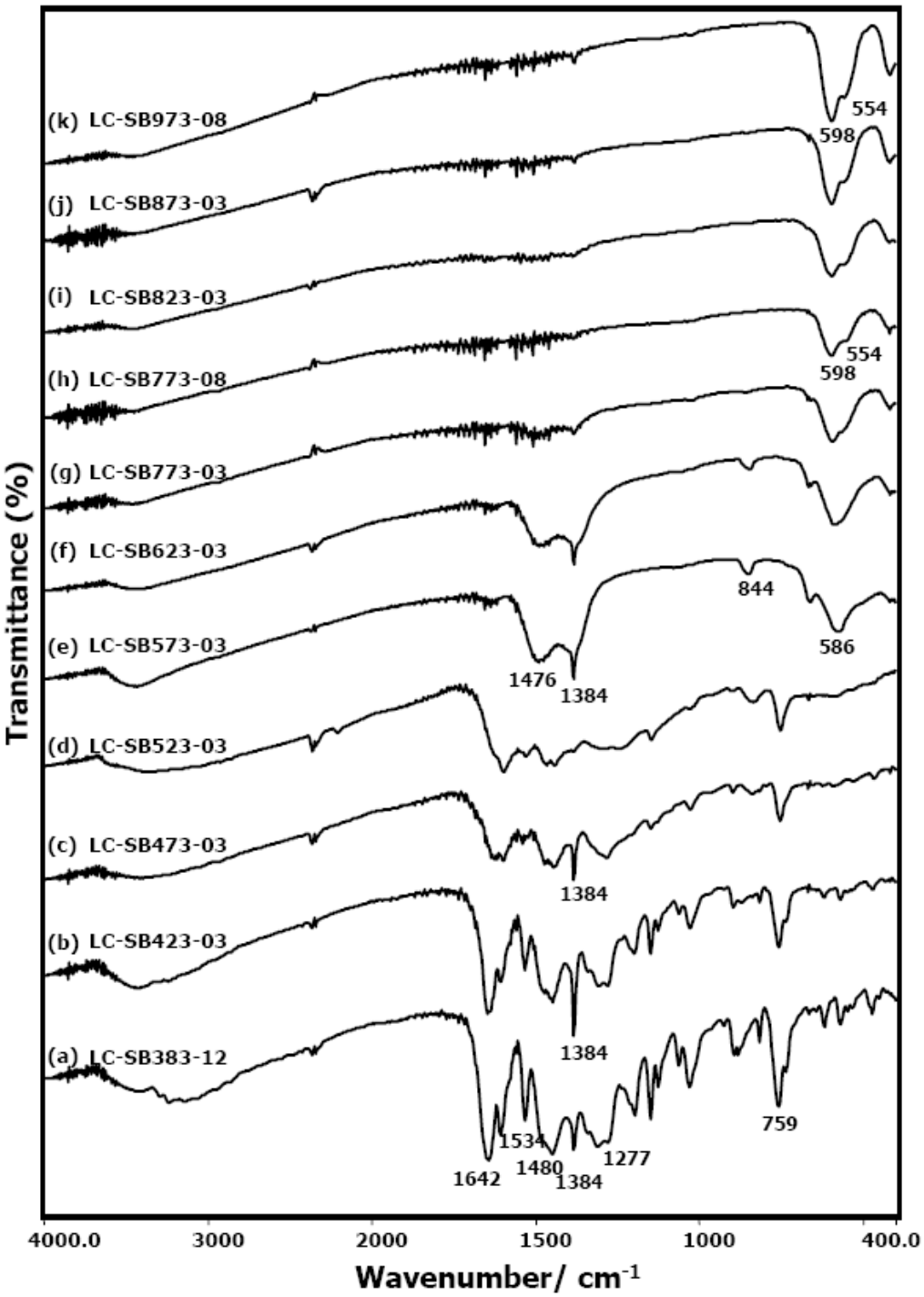

Figure 43 FTIR spectra of the samples prepared by Schiff base complex method at various temperatures

Some selected IR spectral bands are presented in Figure 43. The strong typical absorptions at 1642 cm^{-1} related to the C=N Schiff base imino group.

The band at 1510, 1480 and 1450 cm^{-1} corresponded to the vibration of the C=C stretching in the aromatic ring and medium bands around 1277 cm^{-1} corresponded to O–Ph decreased significantly from 383 K to 523 K [Figure 43(a to d)] due to the combustion of the samples under nitrogen. During the reaction of the gel, reddish-brown gas corresponding to NO_x came out of the sample holder and the N–O stretching at 1384 cm^{-1} of NO_3^- was detected at 383 K till 473 K. LC-SB523-03 exhibited no absorption at 1384 cm^{-1} of NO_3^-. At 573 K, oxygen was applied into the calcinations apparatus which resulted in reforming of some NO_3^- on the surface of LC-SB573-03. It could be assumed that nitrogen from the gel complex, such as C=N functional group, formed NO_3^- producing vacancy on the sample surface ready for adsorbing oxygen in the surrounding gas phase.

When the calcination temperature was increased to 573 K, [Figure 43(e)], the bands due to organic compounds disappeared with bands around 1476, 1364 and 844 cm^{-1} related to the carbonate formation appeared. A Co–O band at 586 cm^{-1} accompanied with a few carbonate is observed. As the dried samples calcined above 773 K, [Figure 43(h)], the bands due to organic compounds disappeared completely and the absorption bands around 598 and 554 cm^{-1} were observed, which corresponded to the existence of Co–O bond stretching. The results proved the formation of $LaCoO_3$.

1.2.3 X-ray Powder diffraction (XRD)

Diffraction data in Table 15 be owned by the peaks of reference and prepared $LaCoO_3$ catalysts which XRD patterns are presented in Figure 44.

Table 15 Diffraction data of $LaCoO_3$ reference and $LaCoO_3$ prepared by Schiff base complex method

Catalysts	2θ	I/I_0	D
$LaCoO_3$	32.91	100	2.72
(JCPDS no: 25-1060)	33.31	95	2.69
	47.52	70	1.91
	59.01	55	1.56
LC-SB573-03	33.19	100.00	2.70
	47.50	49.91	1.91
	58.87	53.20	1.57
LC-SB773-08	33.08	100.00	2.71
	33.39	79.29	2.68
	59.00	52.60	1.56
LC-SB823-08	33.02	98.67	2.71
	33.32	100.00	2.69
	47.59	65.79	1.91
LC-SB973-08	32.96	100.00	2.72
	33.34	99.53	2.69
	47.53	54.89	1.91

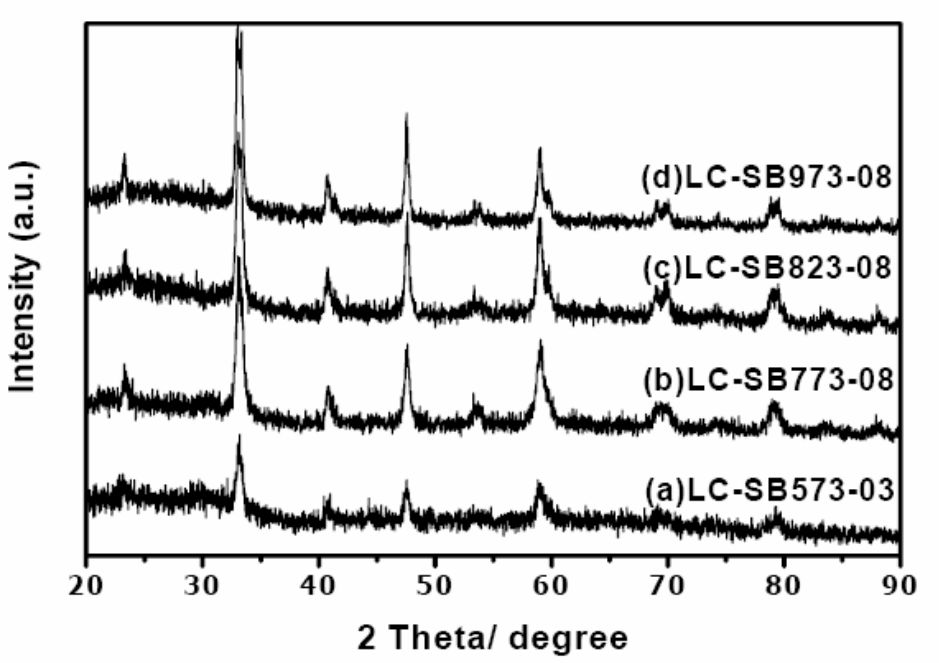

Figure 44 X-ray diffraction patterns of the samples prepared by Schiff base complex method and calcined at various temperatures (a) LC-SB573-03, (b) LC-SB773-08, (c) LC-SB823-08 and (d) LC-SB973-08

A similar crystallization behavior is observed for the powder precursor obtained from the Schiff base complex method, as shown in Figure 44. When LC–SB samples were subjected to the treatment at 573 K for 3 hours [Figure 44(a)], peaks at 33.31˚, 47.65˚ and 59.30˚ due to the $LaCoO_3$ were observed (JCPDS PDF No. 25-1060). However, a broad continuum around 30˚, indicative of the presence of amorphous components, persisted even after raising the calcination temperature from 573 to 773 K and simultaneously extending the heating time from 3 hours to 8 hours [Figure 44(b)]. Complete crystallization now took place at 823 K [Figure 44(c)], and the XRD pattern of the powder treated at 973 K was characteristic of a monophase perovskite with a rhombohedral symmetry, peaks at d-spacing values of 2.72, 2.69 and 1.91, corresponded to the 2θ values 32.96˚, 33.34˚ and 47.53˚ [Figure 44(d)]. Results showed no traces of $La(OH)_3$ [2θ 27.97˚ (JCPDS PDF No. 13-0084)] and Co_3O_4 [2θ 36.94˚ (JCPDS PDF No. 74-1656)].

The calculated value of crystallite size of each calcined samples are shown in Table 16 and the calculation details are shown as follows:

At (h k l) = (0 2 4); 2θ = 47.54˚, thus calculated value of $\beta_{reference}$ due to equation 15 is as follow:

$$\beta_{reference} = 0.0027\, e^{-8\times10^{-4}\times 47.54}$$

$$\beta_{reference} = 2.60\times10^{-3} \text{ radian}$$

The value of FWHM 0.98˚ must be changed into radian unit using observed scale value of 1˚= π/ 180˚ radian. Thus

$$\beta_{observed} = 0.98^\circ \times \frac{\pi}{180^\circ}$$

$$\beta_{observed} = 1.71\times10^{-2} \text{ radian}$$

The true peak breadth, β, in radian unit is given by;

$$\beta = \sqrt{\left(1.71\times10^{-2}\right)^2 - \left(2.60\times10^{-3}\right)^2}$$

$$\beta = 1.69\times10^{-2} \text{ radian} \qquad .....(17)$$

Substitute the value of β in equation 17, k = 0.9 and λ = 1.54 Å into Scherrer equation and crystallite size (D) can be determined as follows:

$$D = \frac{(0.9)(1.54)}{1.69\times10^{-2}\cos 0.42}$$

$$D = 89.85 \text{ Å}$$

$$D = 9.0 \text{ nm}$$

The crystallite sizes of calcined $LaCoO_3$ were 9-27 nm shown in Table 16, calculated by means of x-ray broadening method using Scherrer equations. When the calcination temperature was higher, the crystallite size increased.

Table 16 Calculated values of crystallite sizes of samples prepared by Schiff base complex

Catalysts	2Theta	Theta (radian)	β_s (radian)	FWHM β_m (degree)	β_m (radian)	β (radian)	D (nm)
LC-SB573-03	47.54	0.4148	0.0026	0.98	0.0171	0.0169	9.0
LC-SB773-08	47.60	0.4154	0.0026	0.68	0.0119	0.0116	13.1
LC-SB823-08	47.62	0.4155	0.0026	0.45	0.0079	0.0075	20.2
LC-SB973-08	47.52	0.4147	0.0026	0.36	0.0062	0.0056	26.8

1.3 Coprecipitation (CP)

1.3.1 Thermogravimetric analysis (TGA)

A TG curve of the prepared coprecipitate fired in the temperature range between 303 and 873 K is illustrated in Figure 45.

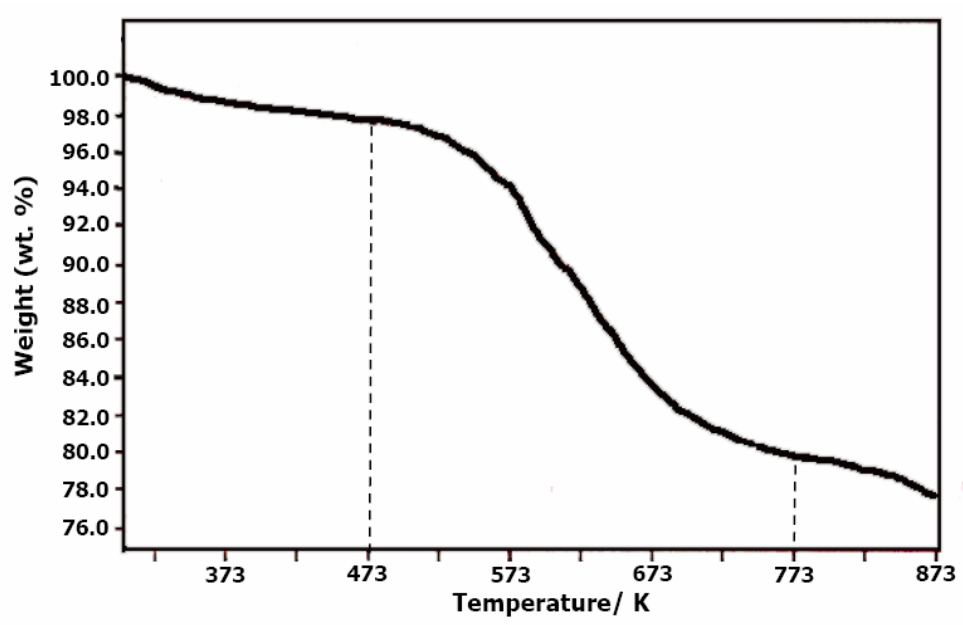

Figure 45 TG curve of the sample prepared by coprecipitation

The weight loss resulted from the heat treatment of the dried LC-CP is shown in the TG curve (Figure 45). The percentage weight started to decrease at approximately 473 K and to be stable at 773 K. The percentage weight loss of the full process suggested that the dried LC-CP lost water from the hydroxide precipitates and nitrate ion mixed as impurity was lost in the form of NO_x. Percentage weight loss was a little at approximately 823 K, thus this temperature was suitable for calcination.

1.3.2 Fourier Transform Infrared Spectroscopy (FTIR)

Data of IR spectra of the coprecipitation are summarized in Table 17 and the spectra are shown in Figure 46.

Table 17 FTIR spectra assignment of samples prepared by coprecipitation

Functional group / Catalysts	Wavenumber (cm^{-1})				
	O–H stretching	O–H bending	N–O bending of nitrate ion	Co–OH stretching	Co–O stretching
Reference	3700-3500[(1)]	1630-1600[(1)]	1384[(b)]	< 1200[(a)]	596, 552[(d)]
LC-CP383-12	3490	1638	1384	1044	-
LC-CP423-03	3490	1638	1384	1044	669, 568
LC-CP773-03	3490	1638	1384	1044	669, 568
LC-CP823-03	-	-	1384	-	669, 577
LC-CP873-03	-	-	1384	-	669, 584
LC-CP973-03	-	-	1384	-	669, 595
LC-CP973-03	-	-	1384	-	669, 595

[(a)] NaKamoto (1997) [(b)] Sinquin *et al.* (2001) [(c)] Khalil (2003)

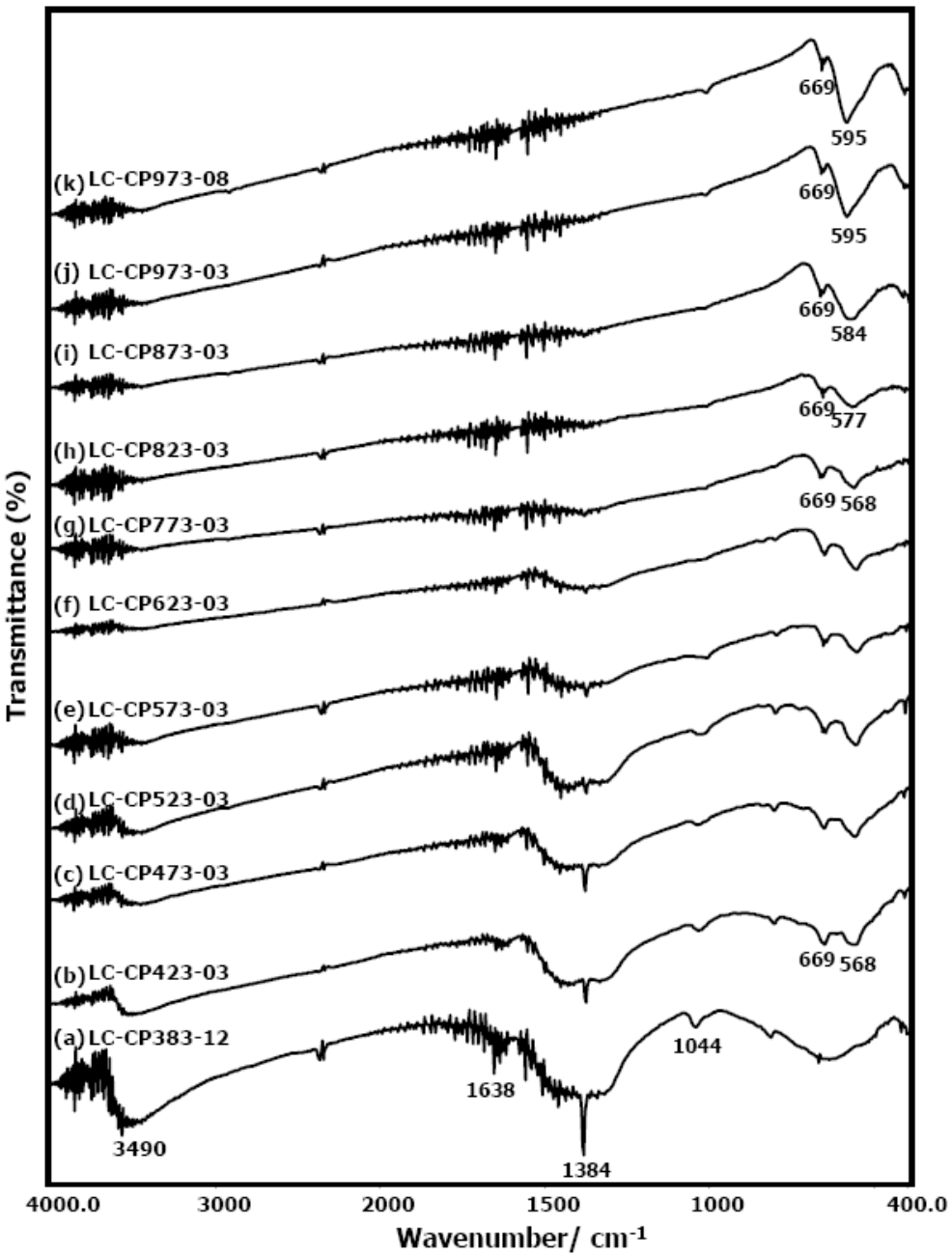

Figure 46 FTIR spectra of the samples prepared by coprecipitation at various temperatures

Figure 46 illustrates IR spectra resulting from heat treatment of $La(OH)_3$ and $Co(OH)_2$ coprecipitates under different conditions. The coprecipitates dried at 383 K in an oven for 12 hours [Figure 46(a)] showed the O–H stretching and O–H bending at 3490 cm^{-1} and 1638 cm^{-1}, respectively (Nakamoto, K., 1997) and N–O stretching at 1384 cm^{-1} due to some trace of the nitrate precursors. In addition, the

band at 1044 cm^{-1} corresponded to Co–OH bending which is confirmed with the reported value that MOH bending mode appears below 1200 cm^{-1} (Nakamoto, 1997). The IR spectra of LC-CP423-03 to LC-CP623-03 [Figure 46(b) to 46(f)] showed Co–O stretches at 568 and 669 cm^{-1} in the same patterns of Co–O stretching in Co_3O_4 [Appendix Figure A1]. From IR spectra of LC-CP623-03 to LC-CP873-03 [Figure 46(f) to 46(i)], cobalt formed Co–O bond in cobalt oxide (Co_3O_4) and transformed to Co–O bond in $LaCoO_3$. The main FTIR bands were observed at 595 cm^{-1} for Co–O in $LaCoO_3$ [Figure 46(j)] after calcination at 973 K.

1.3.3 X-ray Powder diffraction (XRD)

The XRD patterns of LC-CP samples calcined at 773, 823, 873 and 973 K were shown in Figure 47(a) – (e) and the XRD data are summarized in Table 18.

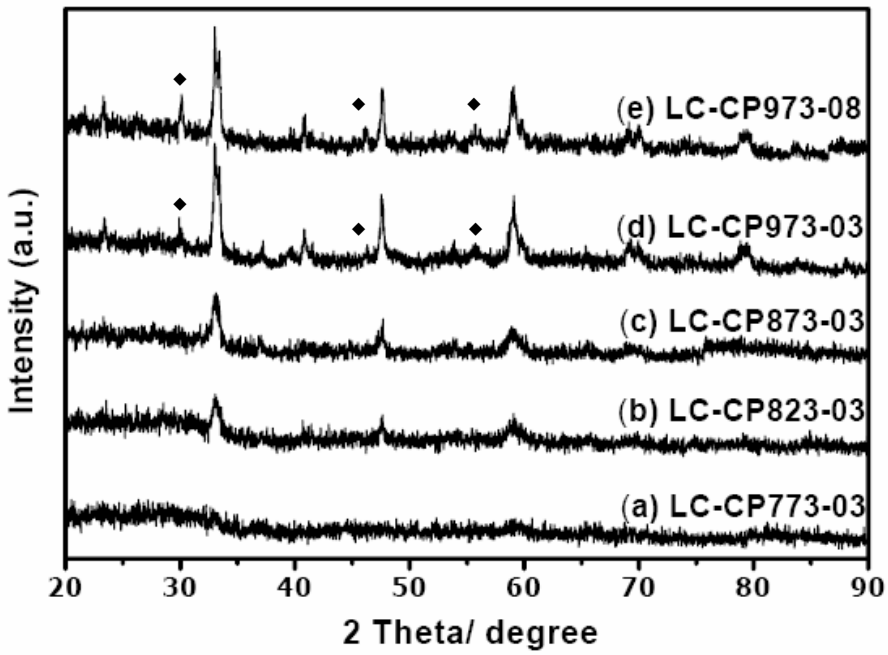

Figure 47 X-ray diffraction patterns of the samples prepared by the coprecipitation and calcined at various temperatures (a) LC-CP773-03, (b) LC-CP823-03, (c) LC-CP873-03, (d) LC-CP973-03 and (e) LC-PN973-08 [◆= $La(OH)_3$]

LC-CP773-03 resulted from the calcination temperature at 723 K showed no perovskite peaks [Figure 47(a)]. The characteristic peaks of perovskite at 2θ 32.91˚, 33.30˚ and 47.50˚ were matched to those perovskite peaks in LC-CP823, 873 and 973 [Figure 47(b-e)]. These results showed that LC-CP823, 873 and 973 were $LaCoO_3$ perovskite with hexagonal symmetry corresponding to JCPDS 25-1060. The XRD of LC-CP973-03 and LC-CP973-08 showed, in addition to perovskite, the presence of peaks at 2θ 24.30˚, 30.15˚ and 43.67˚ corresponding to $La(OH)_3$ (JCPDS 13-0084) as impurity (Table 19).

Table 18 Diffraction data of $LaCoO_3$ reference and $LaCoO_3$ prepared by coprecipitation

Catalysts	2θ	I/I_0	d
$LaCoO_3$	32.91	100	2.72
(JCPDS no: 25-1060)	33.31	95	2.69
	47.52	70	1.91
	59.01	55	1.56
LC-CP773-03	-	-	-
LC-CP823-03	33.02	100.00	2.71
	47.58	50.10	1.91
	58.99	37.63	1.56
LC-CP873-03	33.00	100.00	2.71
	47.70	53.13	1.91
	58.95	45.69	1.57
LC-CP973-03	33.01	100.00	2.71
	33.44	82.75	2.68
	47.61	58.13	1.91
LC-CP973-08	33.02	100.00	2.71
	33.40	82.21	2.68
	47.61	54.96	1.91

Table 19 Diffraction data of $La(OH)_3$ reference and $La(OH)_3$ impurity in $LaCoO_3$ prepared by coprecipitation

Catalysts	2θ	I/I_0	d
$La(OH)_3$	30.15	100	2.96
(JCPDS 13-0084)	24.30	75	3.66
	43.67	61	2.07
LC-CP773-03	-	-	-
LC-CP823-03	-	-	-
LC-CP873-03	-	-	-
LC-CP973-03	29.91	29.51	2.98
	39.59	11.13	2.27
	46.34	7.94	1.96
LC-CP973-08	30.13	26.11	2.96
	40.80	14.49	2.21
	45.24	6.19	2.00

The calculated value of crystallite size of each calcined samples are shown in Table 20 and the calculation details are shown as follows:

At (h k l) = (0 2 4); 2θ = 47.62˚, thus calculated value of $\beta_{reference}$ due to equation 15 is as follow:

$$\beta_{reference} = 0.0027\, e^{-8\times10^{-4}\times 47.62}$$

$$\beta_{reference} = 2.60\times10^{-3} \text{ radian}$$

The value of FWHM 0.52˚ must be changed into radian unit using observed scale value of 1˚= π/ 180˚ radian. Thus

$$\beta_{observed} = 0.52^\circ \times \frac{\pi}{180^\circ}$$

$$\beta_{observed} = 9.08\times10^{-2} \text{ radian}$$

The true peak breadth, β, in radian unit is given by;

$$\beta = \sqrt{\left(9.08\times10^{-2}\right)^2 - \left(2.60\times10^{-3}\right)^2}$$

$$\beta = 8.70\times10^{-2} \text{ radian} \qquad \text{.....(18)}$$

Substitute the value of β in equation 18, k = 0.9 and λ = 1.54 Å into Scherrer equation and crystallite size (D) can be determined as follows:

$$D = \frac{(0.9)(1.54)}{8.70\times10^{-2}\cos 0.42}$$

$$D = 174.42 \text{ Å}$$

$$D = 17.4 \text{ nm}$$

The samples from the coprecipitation started to form perovskite structure at 823 K to produce particles with the size of 17.4 nm. When the calcination temperature increased, the same results as those observed from the Pechini and Schiff base complex method, the crystallite sizes increased.

Table 20 Calculated values of crystallite sizes of samples prepared by coprecipitation

Catalysts	2Theta	Theta (radian)	β_s (radian)	FWHM β_m (degree)	β_m (radian)	β (radian)	D (nm)
LC-CP823-03	47.62	0.4155	0.0026	0.52	0.0091	0.0087	17.4
LC-CP873-03	47.68	0.4161	0.0026	0.47	0.0082	0.0078	19.5
LC-CP973-03	47.64	0.4157	0.0026	0.42	0.0073	0.0068	22.1
LC-CP973-08	47.62	0.4155	0.0026	0.40	0.0071	0.0066	23.1

2. Catalyst Characterization

The samples obtained from the Pechini, the Schiff base complex and the coprecipitation methods were characterized to study the effects of preparations in the perovskite prepared by different methods.

2.1 X-ray photoemission spectroscopy (XPS)

Surface composition of a series of the perovskites prepared by three different methods was studied by XPS. The resulting binding energy values were corrected using C 1s peak at 285 eV. Deconvoluted XPS spectra of La 3d, O 1s and Co 2p are shown in Figure 48 - 20, respectively. Table 21-23 lists the corresponding binding energies of La 3d, Co 2p, and O 1s. The calculated oxygen ratios of OH^-/O^{2-} are summarized in Table 21.

Figure 48 - 49, two peaks of La $3d_{3/2}$ are located at 834.4 – 834.7 and 837.9 – 838.3 eV and those of La $3d_{5/2}$ are at 851.2 – 851.5 and 854.8 – 855.1 eV, respectively, (Table 21). And the spin-orbit splitting of La 3d was 16.8 ± 0.1 eV. These were close to the values recorded for La $3d_{3/2}$ at 851.2 and 855.3 and for La $3d_{5/2}$ at 834.4 and 838.5 with spin-orbit splitting of 16.8 eV were observed (Zhang-Steenwinkel *et al.*, 2002). As might be expected, the data indicate that lanthanum ions are present in the trivalent form for all the samples.

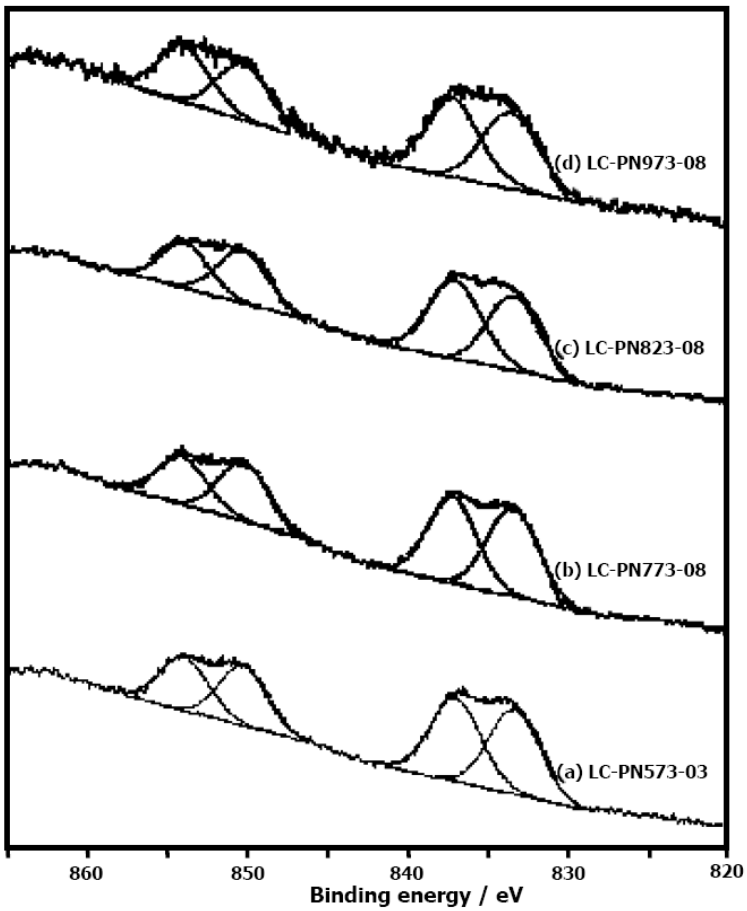

Figure 48 La 3d photoelectron spectra of the samples prepared by the Pechini method

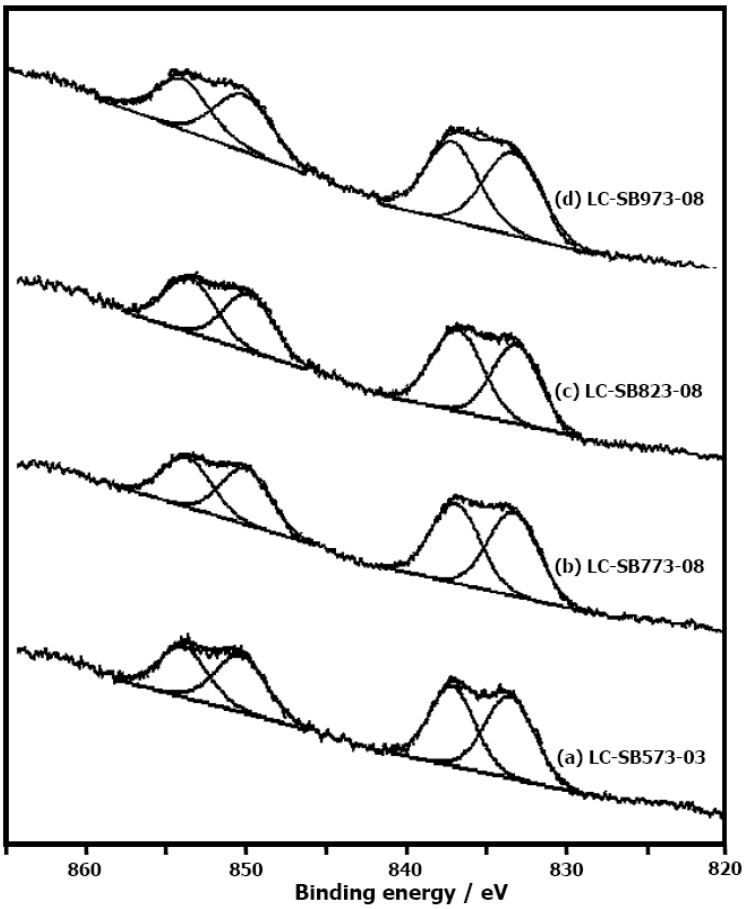

Figure 49 La 3d photoelectron spectra of the samples prepared by Schiff base complex method

Table 21 Binding energies of La 3d of the prepared $LaCoO_3$

Catalyst	La 3d				
	La $3d_{3/2}$		La $3d_{5/2}$		
	Binding energy (eV)	Area	Binding energy (eV)	Area	Spin orbit splitting value (eV)
Reference[(1)]	851.2		834.4		16.8
	855.3		838.5		
LC-PN573-03	851.2	8965.6	834.5	13651.2	16.7
	854.8	9237.9	838.1	13718.7	16.7
LC-PN773-08	851.2	11041.2	834.4	16080.9	16.8
	854.8	9210.9	838.0	17848.7	16.8
LC-PN823-08	851.2	10278.5	834.4	15462.4	16.8
	855.0	8248.7	838.2	14814.5	16.8
LC-PN973-08	851.5	10374.9	834.7	16091.0	16.8
	855.1	9879.4	838.3	15946.9	16.8
LC-SB573-03	851.2	9331.8	834.4	13371.2	16.8
	855.0	8317.8	838.2	12361.7	16.8
LC-SB773-08	850.9	7726.3	834.2	10191.8	16.7
	854.6	7490.0	837.9	11289.7	16.7
LC-SB823-08	851.2	8210.6	834.5	12637.9	16.7
	854.8	7378.9	838.1	11707.1	16.8
LC-SB973-08	851.5	6675.2	834.7	9258.4	16.8
	855.1	5792.0	838.3	8316.0	16.8
LC-CP823-08[(a)]	853.8	98376.1	836.8	160393.6	17.0
	857.4	71611.0	840.6	125825.4	16.8
LC-CP973-08[(a)]	854.7	109914.93	837.7	164457.95	17.0
	858.0	62583.78	841.1	119229.61	16.9

(1) Zhang – Steenwinkel *et al.*, 2002.

(a) Source: Kityakarn (2005)

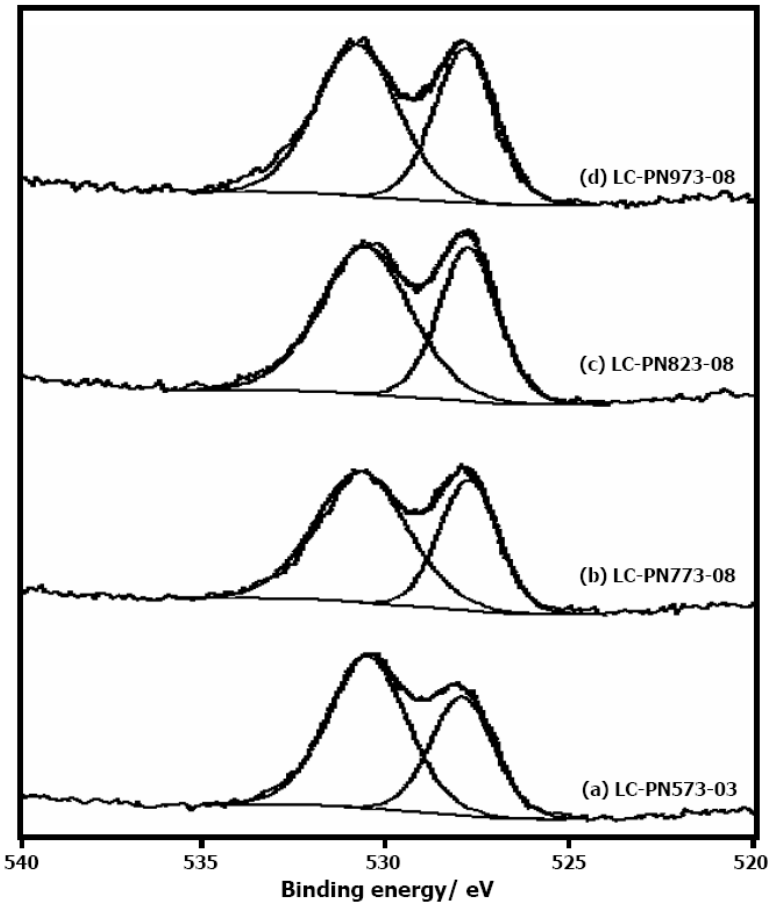

Figure 50 O 1s photoelectron spectra of the samples prepared by the Pechini method

The spectra in Figure 50 - 51 showed asymmetrical O1s XPS peaks. The results revealed that oxygen species existed in mixed oxidation state on the catalysts surface. The relative content of two kinds of oxygen species can be estimated from the relative area of deconvoluted peaks.

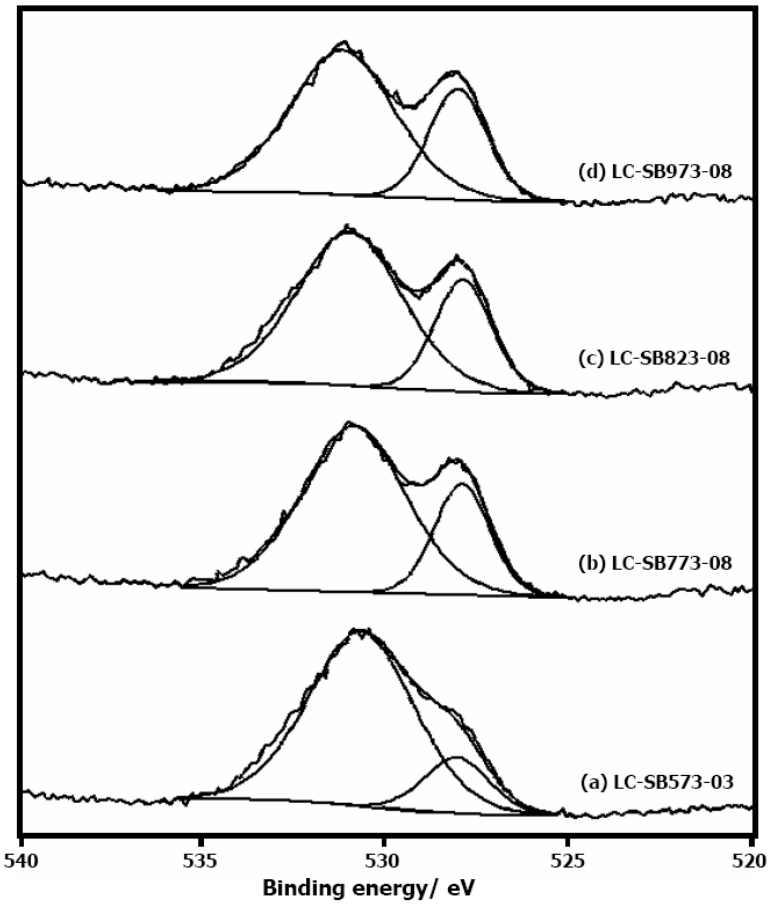

Figure 51 O 1s photoelectron spectra of the samples prepared by Schiff base complex method

Table 22 Binding energies of O 1s of the prepared $LaCoO_3$

Catalyst	O1s		
	Binding energy (eV)	Area	Area ratio
Reference[(1)] O^{2-}	529.0		
OH^-	531.0		
LC-PN573-03	529.0	5396.13	1.61
	531.6	8690.54	
LC-PN773-08	528.8	4934.83	1.58
	531.7	7797.20	
LC-PN823-08	528.7	5535.77	1.48
	531.6	8168.77	
LC-PN973-08	528.8	4791.28	1.26
	531.7	6054.68	
LC-SB573-03	528.9	2311.49	4.61
	531.6	10667.30	
LC-SB773-08	528.7	3498.65	2.83
	531.7	9903.57	
LC-SB823-08	528.6	3664.15	2.55
	531.7	9344.00	
LC-SB973-08	528.7	3689.60	2.42
	531.8	8916.08	
LC-CP823-08[(a)]	530.4	75686.09	1.31
	532.8	99138.48	
LC-CP973-08[(a)]	530.4	66776.99	1.64
	533.2	109574.82	

(1) Zhang – Steenwinkel *et al.*, 2002.

(a) Source: Kityakarn (2005)

Those peaks were assigned to O 1s: a low binding energy (BE) found at 528.2 – 529.0 eV corresponded to the value of at 529.0 eV, which is accepted as lattice oxygen (β-oxygen) in the form of O^{2-}, and a peak at 531.1 – 531.8 eV, corresponded to the reported value of 531.0 eV, which is assigned to the surface adsorbed oxygen (α-oxygen) in the form of CO_3^{2-} or OH^- (Zhang-Steenwinkel *et al.*, 2002). Peaks above 533.0 eV were not observed from the prepared samples, suggesting that these samples do not contain any adsorbed molecular water.

The ratios of adsorbed oxygen (α-oxygen) to lattice oxygen (β-oxygen) are in Table 22. When the calcination temperature increased, the absorbed oxygen to lattice oxygen ratio (α-oxygen/β-oxygen) decreased. The samples prepared by the Schiff base complex method had higher numbers of peak area ratios than those prepared by the Pechini method. The Pechini and the Schiff base complex methods producing organolanthanum and organocobalt complex intermediates made the lanthanum and cobalt ions stable during calcination to form the perovskite structure when the organic ligands decomposed, with less impurity of unreacted metal oxides. It could be confirmed that nitrogen from the Schiff base complex, such as C=N functional group, formed NO_3^- producing vacancy on the sample surface ready for adsorbing oxygen in the surrounding gas phase producing high number of adsorbed oxygen on the sample surface compared to those produced from the Pechini method. The samples prepared by both sol-gel methods had higher numbers of peak area ratios than those prepared by the coprecipitation. This could be explained by a higher diffusion barrier of the La^{3+} and Co^{3+} ions for the samples from the sol-gel method caused by the organic ligand forming less crystallinity of the perovskite with higher ratios of adsorbed oxygen to lattice oxygen.

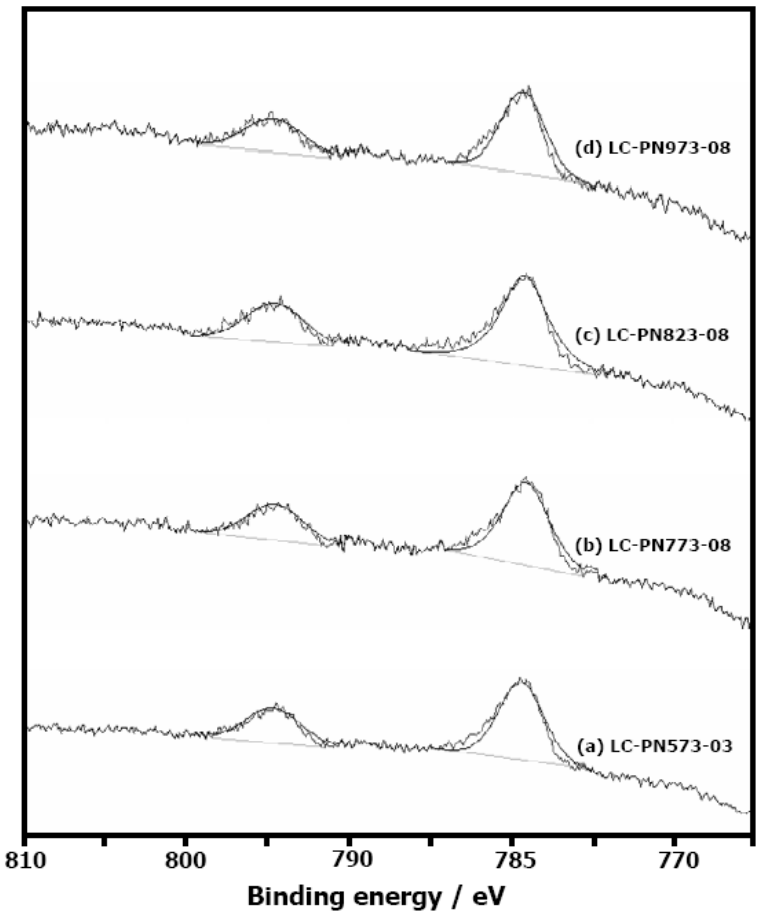

Figure 52 Co 2p photoelectron spectra of the samples prepared by the Pechini method

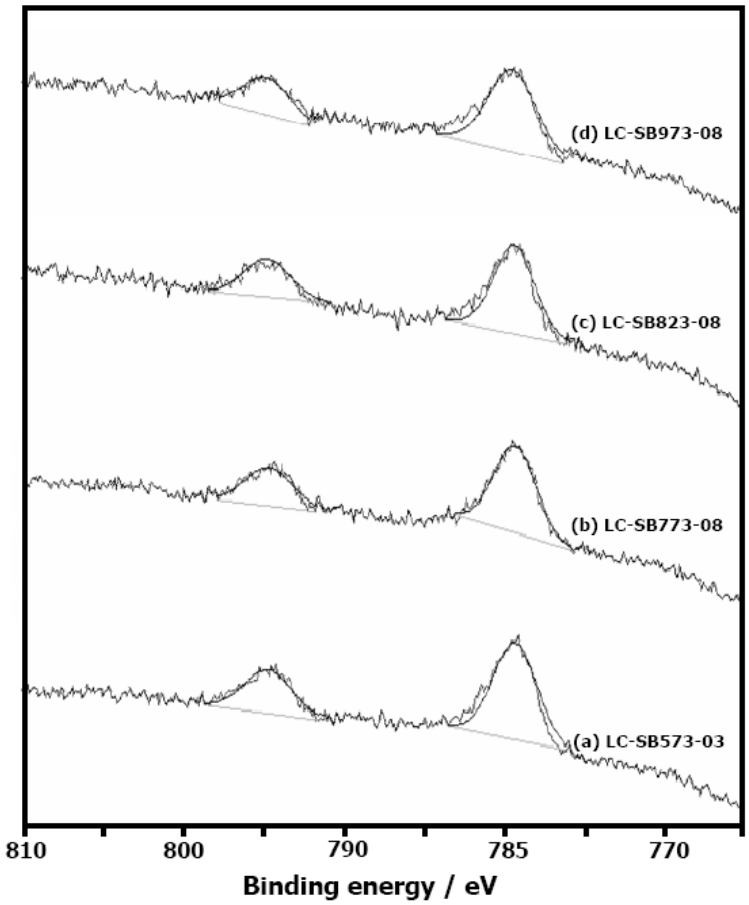

Figure 53 Co 2p photoelectron spectra of the samples prepared by Schiff base complex method

The XPS Co 2p spectra for all samples were similar in shape. The peaks of Co $2p_{3/2}$ and Co $2p_{1/2}$ are located at 780.1 – 780.3 and 795.5 – 795.7 eV (Figure 52 – 53). The spin-orbit splitting of Co 2p was 15.4 eV (779.8±0.3 and 795.0±0.3, respectively), which was in agreement with the literature values for Co^{3+} ions in $LaCoO_3$ (Siem *et al.*, 1997).

Table 23 Binding energies of Co 2p of the prepared $LaCoO_3$

Catalyst	Co 2p				
	Co $2p_{1/2}$		Co $2p_{3/2}$		
	Binding energy (eV)	Area	Binding energy (eV)	Area	Spin orbit splitting value (eV)
Reference[(1)]	779.8±0.3		795.0±0.3		15.4
LC-PN573-03	780.1	4143.6	795.7	2237.9	15.5
LC-PN773-08	780.2	7321.2	795.6	3557.3	15.4
LC-PN823-08	780.3	5747.2	795.7	2834.1	15.4
LC-PN973-08	780.3	6823.6	795.7	3706.0	15.4
LC-SB573-03	780.2	4689.7	795.6	2074.4	15.4
LC-SB773-08	780.2	3966.9	795.6	1884.0	15.4
LC-SB823-08	780.2	4347.0	795.5	2183.8	15.3
LC-SB973-08	780.2	5103.2	795.6	2559.9	15.4

(1) Siem *et al.*, 1997.

The results binding energy values were corrected using C 1s peak at 285.0 eV. The C 1s spectra, Appendix Figure B1 – B3, showed two peaks at 285.0 eV and 288.5 - 289.2 eV, which closed to 289.2 eV, caused by the presence of surface carbonates (Zhang-Steenwinkel *et al.*, 2002).

2.2 X-ray fluorescence spectroscopy (XRF)

The theoretical values of percentage weight of elements in $LaCoO_3$ and experiment XRF results of the samples prepared by the Pechini and the Schiff base complex methods are reported in Table 24.

Calculation of percentage weight of elements in $LaCoO_3$ unit cell

The mole ratio of La:Co in $LaCoO_3$ perovskite unit cell is 1:1 (Molecular weight of La and Co are 138.91 and 58.93 g mol^{-1}, respectively).

$$\text{Percentage weight of La in a perovskite unit cell} = \frac{1 \times 138.91}{138.91 + 58.93} \times 100$$

$$= 70.21\ \%$$

$$\text{Percentage weight of Co in a perovskite unit cell} = \frac{1 \times 58.93}{138.91 + 58.93} \times 100$$

$$= 29.79\ \%$$

Table 24 The XRF results of the prepared $LaCoO_3$

Catalyst	% weight	
	La	Co
Theoretical values	70.21	29.79
LC-PN973-08	73.83	26.17
LC-SB973-08	72.95	27.95

The content (weight %) of La in LC-PN and LC-SB calcined at 973 K determined by XRF were 73.83 and 72.95, respectively, to be compared with the theoretical value of 70.21. The content of Co in LC-PN and LC-SB calcined at 973 K were 26.17 and 27.95, respectively, to be compared with the theoretical value of 29.79. The contents of La and Co were corresponded to the theory calculation and the molar ratio of La:Co was 1:1 as in one unit cell.

2.3 Nitrogen adsorption by Brumett - Elmer (BET) method

The surface areas of $LaCoO_3$ powders prepared at 573, 773, 823 and 973 K by the Pechini and the Schiff base complex methods are listed in Table 25.

Table 25 Surface area of the prepared $LaCoO_3$

Catalyst	Surface area (m^2g^{-1})
LC-PN573-03	5.88
LC-PN773-08	7.74
LC-PN823-08	7.21
LC-PN973-08	2.84
LC-SB573-03	24.66
LC-SB773-08	11.68
LC-SB823-08	7.80
LC-SB973-08	4.44

The samples from the Pechini procedure showed the surface area of 3 – 7 m^2g^{-1} and those from the Schiff base complex with the value of 4 – 25 m^2g^{-1}. LC-SB had the higher surface area than LC-PN at the same temperature and the surface areas of catalysts depended on the calcination temperature. From the results of the crystallite sizes and the surface areas confirmed that grain growth occurred at high temperature.

3. Catalytic Activity

To determine the effect of structure on the activity of toluene oxidation, perovskite oxides prepared by different methods were studied: LC-PN and LC-SB. Catalytic oxidation of toluene was used as representative reaction.

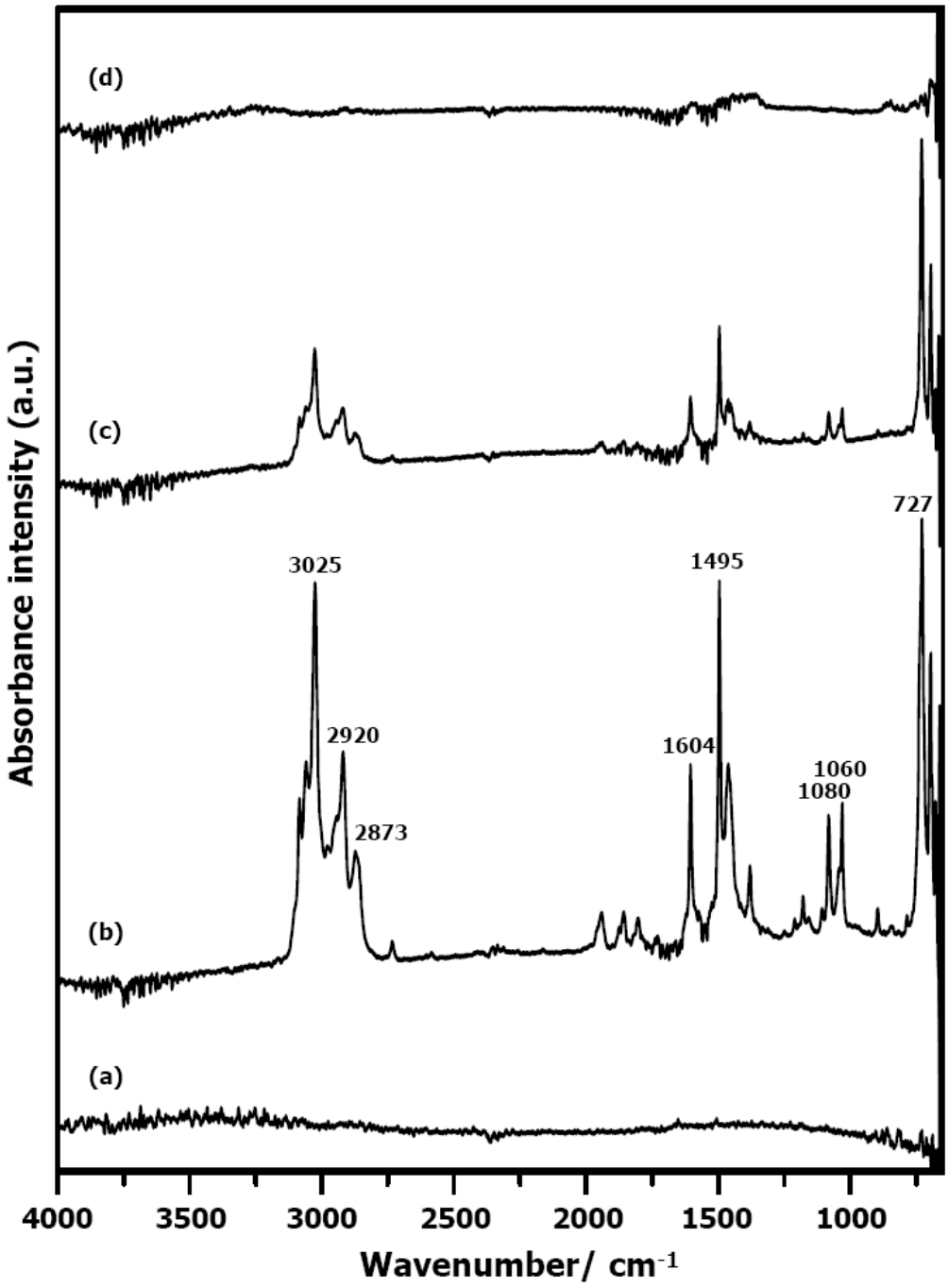

Figure 54 *In situ* infrared spectra of LC-PN773-08 at 423 K: (a) after pretreated 1 hour, (b) before start oxidation, (c) during oxidation reaction at 20 minutes and (d) after evacuation for 10 minutes

Table 26 DRIFTS spectra assignment of LC-PN773-08 catalyst

Wavenumber (cm^{-1})		Functional group
Reference	Observed	
3026[(a)]	3025	C–H stretching in aromatic ring
2921, 2872[(a)]	2920, 2873	asymmetric and symmetric C–H stretching of the methyl group
2000 - 1700[(a)]	2000 - 1700	Overtones of aromatic ring
1604, 1495[(a)]	1604, 1495	C–C stretching in aromatic ring
1379[(a)]	1379	C–H bending of the methyl group
1081, 1061[(a)]	1080, 1060	in plane C–H bending of aromatic ring
728[(a)]	727	out of plane C–H bending of monosubstituted aromatics

[(a)] Poucher (1985)

In Figure 54(a), DRIFTS spectrum of LC-PN773-08 pretreated with Ar/O_2 is shown. No absorption band was observed on catalyst surface. After toluene vapor was passed into the environmental chamber at 423 K, holding it for 30 min and flowing argon was used to remove excess toluene vapor, the bands due to toluene adsorbed on $LaCoO_3$ perovskite surface could be noticed [Figure 54(b)]. Table 26 shows the assignment of the observed bands. The characteristic bands of the adsorbed toluene at 3027 (C–H stretching of aromatic rings) and 2920 and 2873 cm^{-1} (asymmetric and symmetric C–H stretching of the methyl group, respectively) are

observed. A similar spectrum of toluene has been reported in reference (Poucher, 1985), showing the C–H stretching of aromatic rings at 3026 cm^{-1} and the C–H stretch of the methyl group at 2921 cm^{-1}. The C–C stretching of the aromatic rings appeared at 1604 and 1495 cm^{-1} as compared with 1604 and 1495 cm^{-1} in the reference (Poucher, 1985). The C–H bending of the methyl group of toluene was observed at 1080 and 1060 cm^{-1}, as compared with the reference values 1081 and 1061 cm^{-1} (Poucher, 1985).

After Ar/O_2 gaseous mixture was introduced into the environmental chamber, the intensity of the adsorbed toluene band decreased and the band positioned around 3200 cm^{-1} occurred, as shown Figure 54(c). This band, assigned to O–H stretching mode of hydroxide or water, was observed in Figure 54(d) after evacuation at the end of oxidation reaction. However, CH_3OH was observed as an oxidized product from the catalytic oxidation of toluene in the presence of $LaCoO_3$ (Ausadasuk, 2005).

Conversion of the adsorbed toluene as a function of time has been investigated as ratios of the toluene absorption band of the actual time related to that of zero time. The band at 2920 cm^{-1}, which is assigned to asymmetric C–H stretch of methyl group of the adsorbed toluene, used to investigate the toluene conversion over the catalyst. The reaction time used to convert the absorbed toluene to 90% related to that of zero time is shown in Table 27**.**

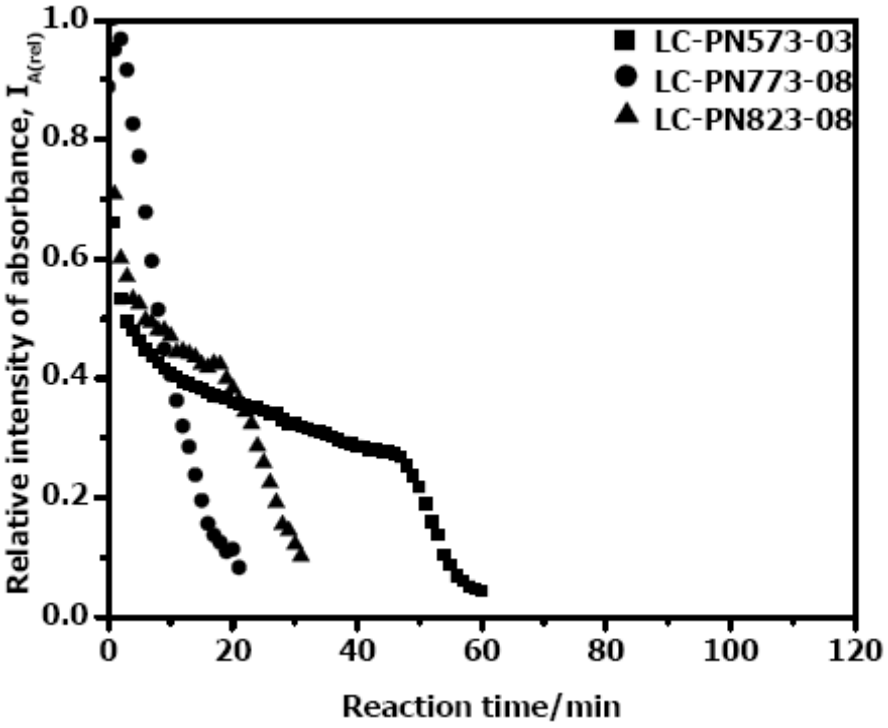

Figure 55 Absorbance intensity at wavenumber 2920 cm^{-1} of the unconverted toluene relative to the starting toluene from oxidation at 423 K on ■ LC-PN573-03, ● LC-PN773-08, ▲ LC-PN823-08 as function of time

Figure 55 shows the absorbance intensity ratio at 2920 cm^{-1} of the unconverted toluene in oxidation reaction relative to the starting toluene as a function of the reaction time in the presence of LC-PN573-03, LC-PN773-08 and LC-PN823-08. LC-PN773-08 converted toluene much faster than those prepared by the Pechini method according to decrease of the absorbance intensity ratio to about 0.10 at 19 minutes. LC-PN573-03 and LC-PN823-08 oxidized toluene to the ratio of 0.10 within 55 and 31 minutes, respectively.

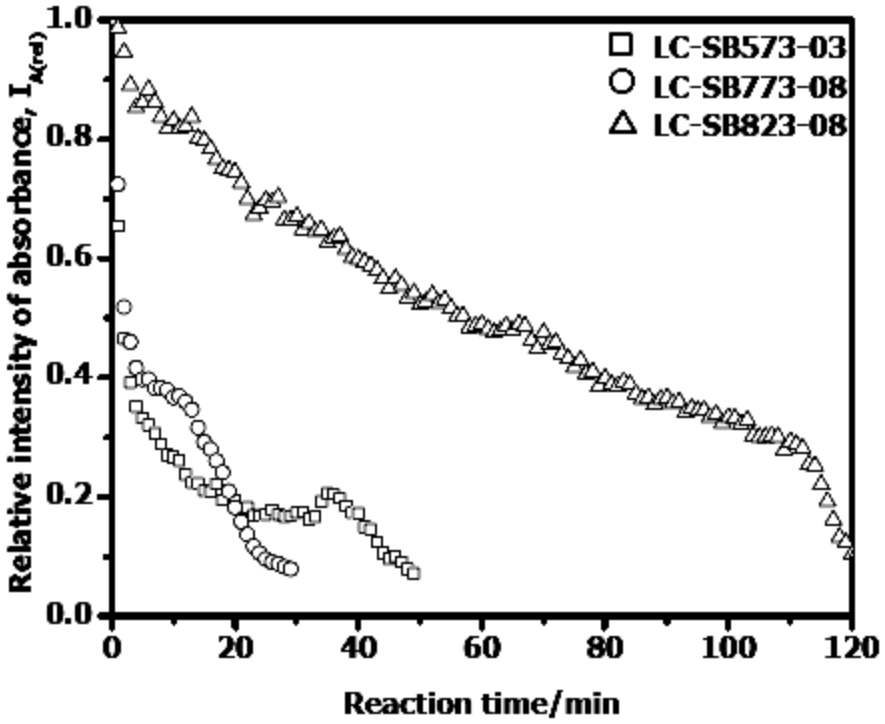

Figure 56 Absorbance intensity at wavenumber 2920 cm^{-1} of the unconverted toluene relative to the starting toluene from oxidation at 423 K on □ LC-SB573-03, ○ LC-SB773-08, △ LC-SB823-08 as function of time

The same comparison has been done for those perovskites prepared by the Schiff base complex method. Figure 56 shows the results, LC-SB773-08 performed well with the observed catalytic activity in terms of the decreasing absorbance intensity ratio at 2920 cm^{-1} of the unconverted toluene relative to the starting toluene to 0.10 within 25 minutes. LC-SB573-03 and LC- SB823-08 oxidized toluene to the ratio 0.10 within 45 minutes and 120 minutes, respectively. It could be concluded that LC-SB773-08 had the best performance between those perovskites prepared by the Schiff base complex method.

Table 27 The time used to convert toluene to 90% related to that of zero time

Catalyst	Crystallite size (nm)	α-oxygen/ β-oxygen	Reaction time (min)
LC-PN573-03	7.5	1.61	55
LC-PN773-08	12.3	1.58	19
LC-PN823-08	18.5	1.48	31
LC-SB573-03	9.0	4.61	45
LC-SB773-03	13.1	2.83	25
LC-SB823-08	20.1	2.55	120

From IR and XRD results, of the three catalysts prepared from the Pechini method, LC-PN573-03 with the smallest crystallite size but still mixed with impurity was poorly active. The sample LC-PN773-08 with the crystallite size of 12.3 nm converted the adsorbed toluene already within 19 min, much faster than the sample LC-PN823-08 with the crystallite size of 18.5 nm.

Apart from the crystallite size of catalysts led to the decreasing in the activity of toluene oxidation. The catalytic reactions were supposed to occur on the $LaCoO_3$ perovskite surface. The XPS results show that increasing the calcination temperature reduces the ratios of adsorbed oxygen to lattice oxygen (α-oxygen/ β-oxygen) shown in Table 27. When further heating the catalyst up to 823 K, the α-oxygen/ β-oxygen strongly decreased. This could be the reason for the decreasing of activity of toluene oxidation indicating that the catalyst with high α-oxygen/ β-oxygen performed well. The same reason has been observed for the samples prepared by the Schiff base complex method.

To compare the effect of different approaches of the both sol-gel preparation on the activity of the perovskites, catalysts calcined at 773 K (LC-PN773-08 and LC-SB773-08) were used. For more exactly, the catalysts were employed to oxidize

toluene at lower temperature of 383 K. The results of toluene oxidation at 393 K are shown in Figure 57.

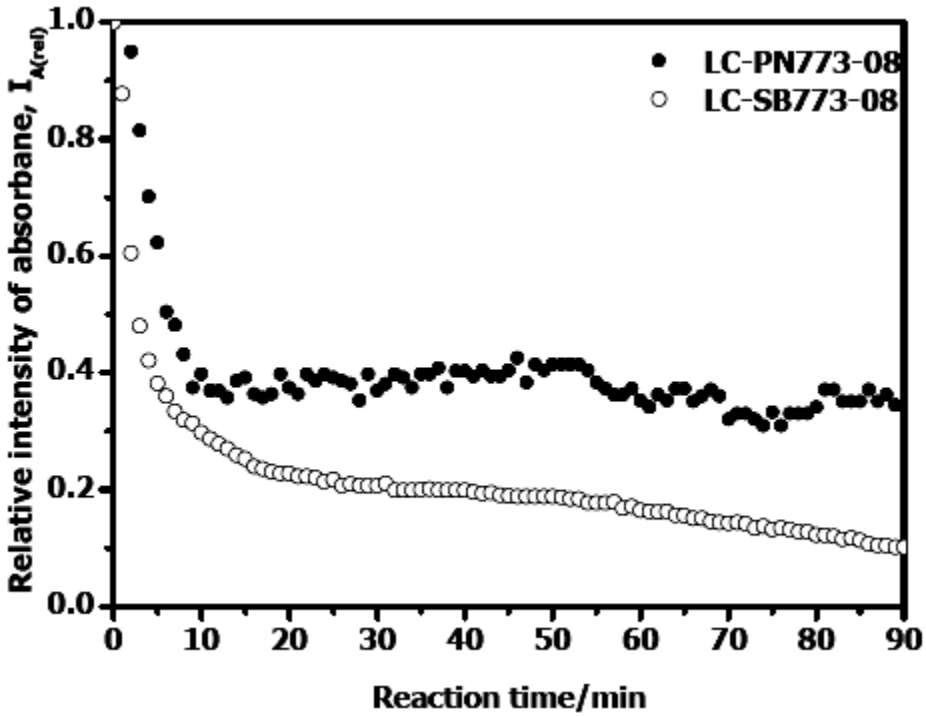

Figure 57 Absorbance intensity at wavenumber 2920 cm^{-1} of the unconverted toluene relative to the starting toluene from oxidation at 393 K on ● LC-PN773-08 and ○ LC-SB773-08 as function of time

The catalysts prepared from the Pechini and Schiff base complex methods showed two periods of oxidation. During the first 7-10 minutes, they had high activity. From ca. 10 minutes their activities were lower and almost constant until 90 minutes reaction time. The reason could be that during the first 10 minutes period, the α-oxygen provides for the oxidation. During the second period, the β-oxygen site is used and it is not reoxidized easily. However LC-SB773 prepared by the Schiff base complex converted the adsorbed toluene faster than LC-PN773 prepared by the Pechini (oxidized the adsorbed toluene to smaller amount).

The results of the toluene oxidation on $LaCoO_3$ can be discussed in terms of redox reaction between toluene and the adsorbed oxygen on the surface of the

perovskite. Zhang *et al.* (2005) proposed that the lattice deficient sites of oxide catalysts influenced the activation and migration of oxygen species as the sequence: $O_{2(gas)} <=> O_{2(surface)} => O_2^-{}_{(surface)} => O_2^{2-}{}_{(surface)} <=> O^-{}_{(surface)} => O^{2-}{}_{(lattice)}$. The properties such as reducibility and oxygen species (lattice oxygen O^{2-} and adsorbed oxygen species O^-) play important roles on the catalytic performance in the oxidation of hydrocarbon. The oxygen close to the Co(III) has been assumed to be transferred to the carbon of the methyl group in toluene producing oxidized compounds. The catalyst LC-SB exhibited high ratio of adsorbed α-oxygen to lattice β-oxygen of 2.83 (Table 27).

The catalytic activity of $LaCoO_3$ perovskite was studied by DRIFTS technique and the catalytic oxidation products of toluene such as methanol and benzaldehyde, which have been detected (Ausadasuk, 2005). The mechanism of the catalytic oxidation of toluene on a $LaCoO_3$ perovskite is proposed by Kityakarn, 2005 as followed:

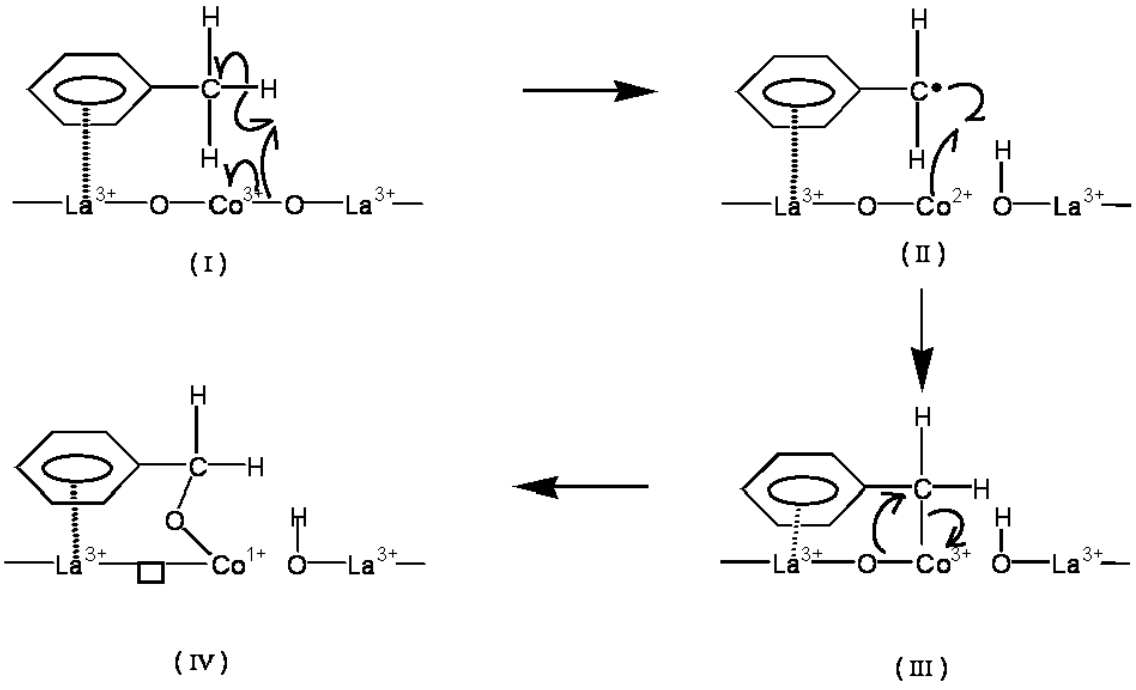

From(IV), the reaction can undergo 3 pathways.

The first pathway:

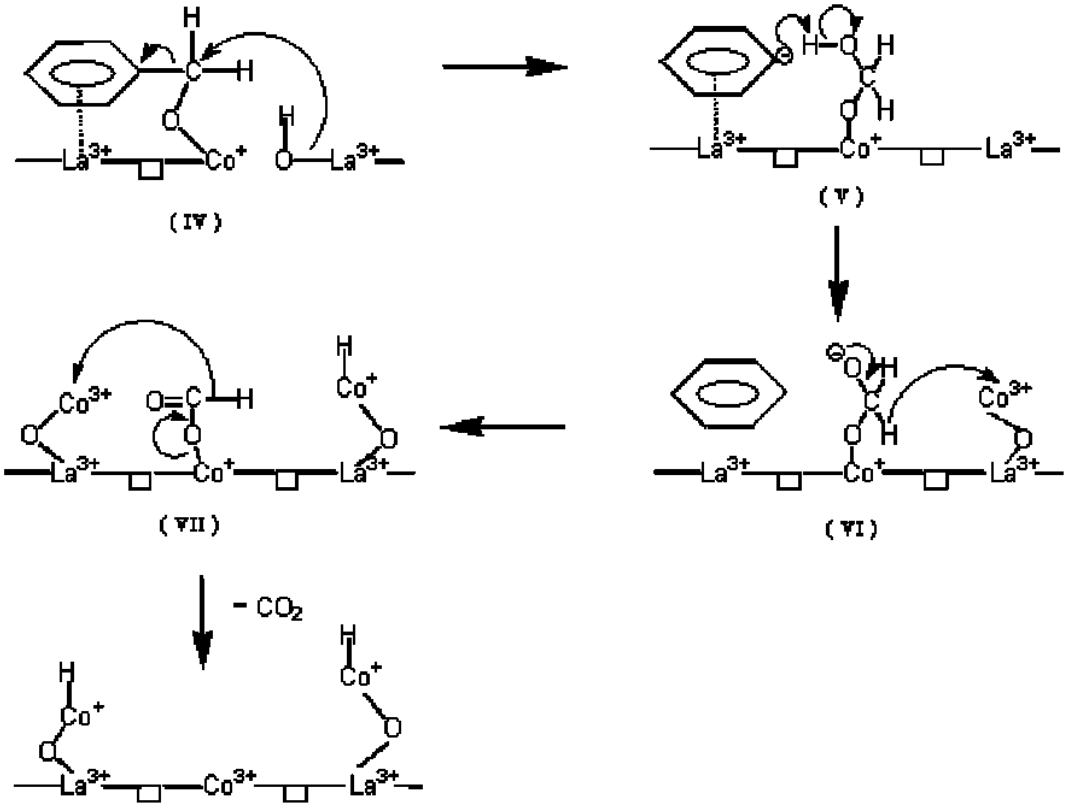

The second pathway:

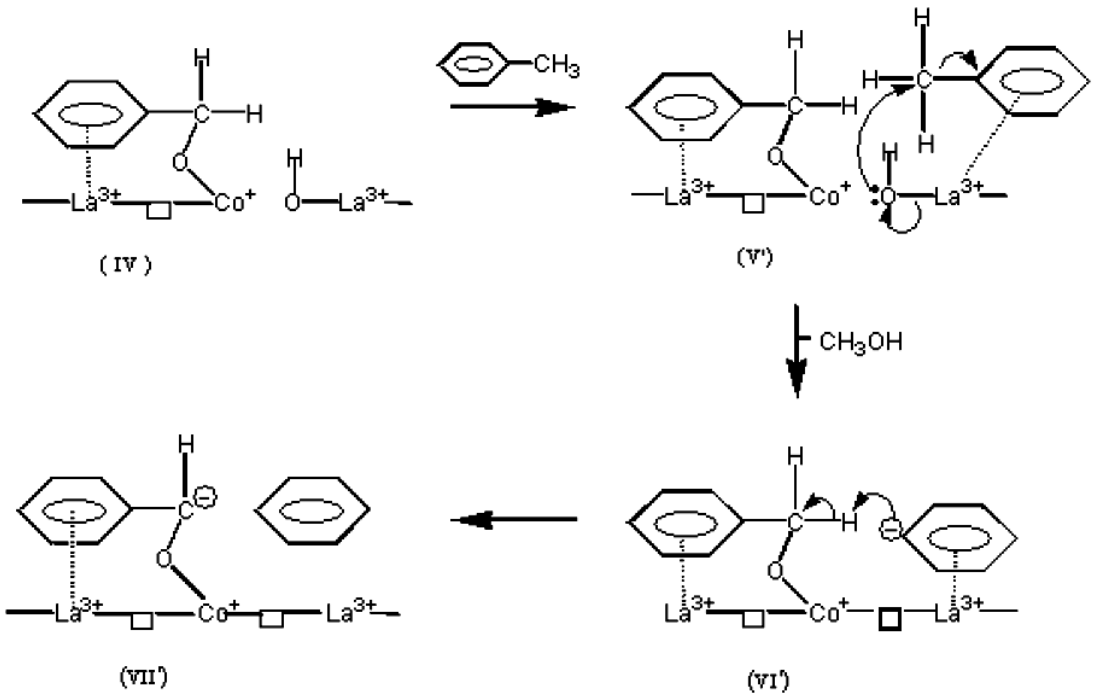

The third pathway:

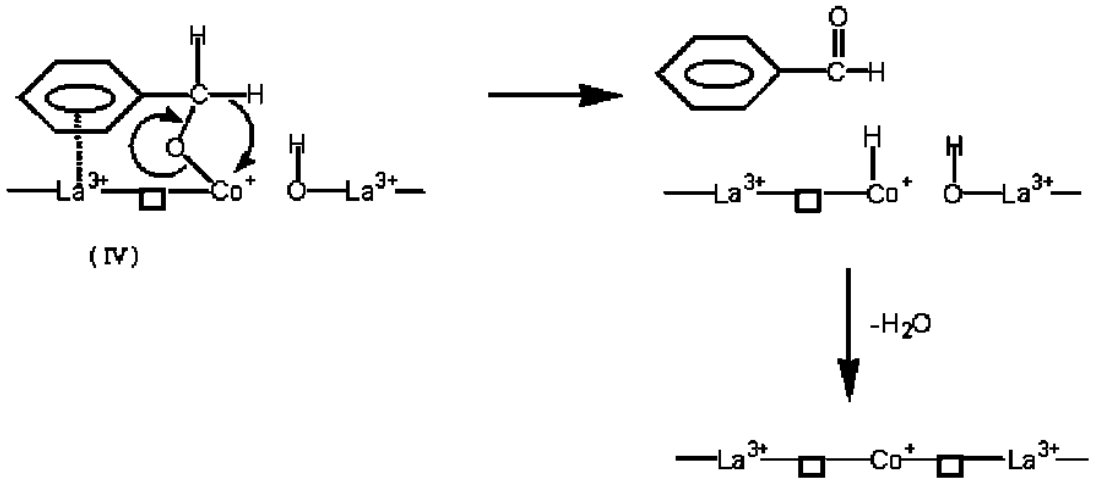

Figure 58 The proposed mechanism of toluene oxidation
Source: Ausadasuk (2005)

In Figure 58, it can be assumed that the reaction proceeds via a mechanism of Mars Van Kevelen type (Grzybowska-Świerkosz, 1997), based on the idea that the reaction of hydrocarbon occurs with oxygen on catalyst only and the vacancies in the oxide network after reaction are reoxidized by oxygen from the gas phase (Zhang *et al.*, 2005). The active species of perovskite, $LaCoO_3$ is Co^{3+} which is active for transferring electron and the surface oxygen (α-oxygen) can be more mobile than lattice oxygen (β-oxygen). In the first step, toluene is adsorbed to La^{3+} site of the perovskite catalyst via π-electron of the benzene ring as physical adsorption (I). The surface oxygen (α-oxygen) is active for cleavage of C-H bond of methyl of toluene forming OH group and π-complex benzyl radical species (II) (Andersson, 1986) which occurs oxidative addition to Co forming (III). The oxygen between La^{3+} and Co^{3+} attacks at the side chain carbon to form adsorbed species (IV). The next step, the reaction can undergo 3 pathways. The first pathway, the α-carbon of methyl group from the adsorbed species (IV) is attacked by OH^-, the C-C bond between benzene ring and methyl is broken and forms (V). The benzyne ion abstracts proton from the adsorbed species (V) and benzene is formed (VI). The next step, carboxylate (VII) is formed on the surface and finally CO_2 is produced and released from the surface. The

second pathway, the other toluene molecule is adsorbed on vicinal La^{3+} site, OH^- attacks the methyl group of toluene. Then benzyne ion is formed and methanol is released. The benzyne ion abstracts proton from α–carbon of the adsorbed species. Benzene is subsequently desorbed and adsorbed species (VII') is formed. The third pathway, water is lost while benzaldehyde is formed and desorbed from the surface. Under the atmosphere of air, the catalyst surface is oxidized by oxygen forming the active perovskite and starts absorbing toluene as in (I).

From the proposed mechanism illustrates that Co^{3+} is reduced to Co^{2+} in step (1) then an oxidative addition occurs to produce Co^{3+}. An α-oxygen between La-O-Co attacks the α-carbon of the methyl group of toluene resulting Co^+ as the adsorbed intermediate (IV). The rates depend on the ability of transferring electrons which involves in changing of electron configurations of the transition metals (Co) in the perovskite. The high oxidation states of the transition metals are found in combination with hard ligands such as oxide. Co (III) configuration $(t_{2g})^6$ is mostly found (Porta *et al.,* 1999), leading to an easy change from the high spin Co (II) configuration $(t_{2g})^5$ $(e_g)^2$ to the low spin Co (III) configuration $(t_{2g})^6$. The reverse reductions of $LaCoO_3$ are changed from Co (III) configuration $(t_{2g})^6$ to Co (II) configuration $(t_{2g})^5$ $(e_g)^2$ and to Co (I) configurations $(t_{2g})^6$ $(e_g)^2$: in case that it reacts with a strong reducing agent such as toluene and an oxide ion such as the α–oxygen in the La-O-Co bond.